Permafrost and Periglacial Processes

WILEY

REVIEW ARTICLE OPEN ACCESS

Developments in Permafrost Science and Engineering in Response to Climate Warming in Circumpolar and High Mountain Regions, 2019–2024

Christopher R. Burn[1] | Annett Bartsch[2] | Elora Chakraborty[3] | Soumik Das[3] | Regula Frauenfelder[4] | Isabelle Gärtner-Roer[5] | Kjersti G. Gisnås[6] | Teddi Herring[7] | Benjamin M. Jones[8] | Steven V. Kokelj[9] | Moritz Langer[10] | Emma Lathrop[11] | Julian B. Murton[12] | David M. Nielsen[13] | Fujun Niu[14] | Christine Olson[15] | H. Brendan O'Neill[16] | Sophie Opfergelt[17] | Pier Paul Overduin[18] | Kevin Schaefer[15] | Edward A. G. Schuur[11] | Elliott Skierszkan[19] | Sharon L. Smith[16] | Simone M. Stuenzi[18] | Suzanne E. Tank[20] | Jurjen van der Sluijs[21] | Gonçalo Vieira[22] | Sebastian Westermann[4] | Stephen A. Wolfe[16] | Ed Yarmak[23]

[1]Department of Geography and Environmental Studies, Carleton University, Ottawa, Ontario, Canada | [2]b.geos GmbH, Korneuburg, Austria | [3]Centre for the Study of Regional Development, Jawaharlal Nehru University, New Delhi, India | [4]Department of Geosciences, University of Oslo, Oslo, Norway | [5]Department of Geography, University of Zurich, Zurich, Switzerland | [6]Natural Hazards Division, Norwegian Geotechnical Institute, Oslo, Norway | [7]Department of Civil Engineering, University of Calgary, Calgary, Alberta, Canada | [8]Institute of Northern Engineering, University of Alaska Fairbanks, Fairbanks, Alaska, USA | [9]Northwest Territories Geological Survey, Government of the Northwest Territories, Yellowknife, Northwest Territories, Canada | [10]Department of Earth Sciences, Vrije Universiteit Amsterdam, Amsterdam, The Netherlands | [11]Center for Ecosystem Science and Society, Northern Arizona University, Flagstaff, Arizona, USA | [12]Department of Geography, University of Sussex, Brighton, UK | [13]Climate Variability Department, Max Planck Institute for Meteorology, Hamburg, Germany | [14]State Key Laboratory of Frozen Soils Engineering, Northwest Institute of Eco-Environment and Resources, Chinese Academy of Sciences, Lanzhou, China | [15]National Snow and Ice Data Center, University of Colorado, Boulder, Colorado, USA | [16]Natural Resources Canada, Geological Survey of Canada, Ottawa, Ontario, Canada | [17]Earth and Life Institute, UCLouvain, Louvain-la-Neuve, Belgium | [18]Permafrost Section, Alfred Wegener Institute, Helmholtz Center for Polar and Marine Research, Potsdam, Germany | [19]Department of Earth Sciences, Carleton University, Ottawa, Ontario, Canada | [20]Department of Biological Sciences, University of Alberta, Edmonton, Alberta, Canada | [21]NWT Centre for Geomatics, Government of the Northwest Territories, Yellowknife, Northwest Territories, Canada | [22]Centre of Geographical Studies, Associate Laboratory Terra, Institute of Geography and Spatial Planning, University of Lisbon, Lisbon, Portugal | [23]Arctic Foundations Inc., Anchorage, Alaska, USA

Correspondence: Christopher R. Burn (christopher.burn@carleton.ca)

Received: 10 May 2024 | **Revised:** 9 October 2024 | **Accepted:** 2 November 2024

Funding: This work was supported by the International Permafrost Association and Carleton University.

Keywords: geochemical contamination | greenhouse gas emissions | ground ice | infrastructure stability | permafrost thaw | thermokarst

ABSTRACT

Research in geocryology is currently principally concerned with the effects of climate change on permafrost terrain. The motivations for most of the research are (1) quantification of the anticipated net emissions of CO_2 and CH_4 from warming and thaw of near-surface permafrost and (2) mitigation of effects on infrastructure of such warming and thaw. Some of the effects, such as increases in ground temperature or active-layer thickness, have been observed for several decades. Landforms that are sensitive to creep deformation are moving more quickly as a result, and *Rock Glacier Velocity* is now part of the Essential Climate Variable *Permafrost* of the Global Climate Observing System. Other effects, for example, the occurrence of physical disturbances associated with thawing permafrost, particularly the development of thaw slumps, have noticeably increased since 2010. Still, others, such as erosion of sedimentary permafrost coasts, have accelerated. Geochemical effects in groundwater from trace elements, including contaminants, and those that issue from the release of sediment particles during mass wasting have become evident

since 2020. Net release of CO_2 and CH_4 from thawing permafrost is anticipated within two decades and, worldwide, may reach emissions that are equivalent to a large industrial economy. The most immediate local concerns are for waste disposal pits that were constructed on the premise that permafrost would be an effective and permanent containment medium. This assumption is no longer valid at many contaminated sites. The role of ground ice in conditioning responses to changes in the thermal or hydrological regimes of permafrost has re-emphasized the importance of regional conditions, particularly landscape history, when applying research results to practical problems.

1 | Introduction

A remarkable transformation of permafrost science and engineering has occurred in the last 15 years, for the real-time effects of climate change on permafrost are now emphasized in most geocryological reports [1, 2]. The rate of publication has exponentially increased [3, 4], and it is almost impossible to maintain universal familiarity with this literature and its rapid developments. Permafrost science has become multidisciplinary, with its geotechnical, geophysical, and geographical basis expanding to include biology, geochemistry, global-scale numerical simulation, and other manifestations of data science.

Two important developments stand out. First, mapping, using remotely sensed imagery of disturbances in permafrost landscapes along with a demonstration of the influence of particularly warm seasons on thermokarst initiation over large areas, has made clear the character, spatial scale, spatial density, and pace of the permafrost responses to climate change [5, 6]. The responses vary from landscape to landscape and region to region. Second, the progress in quantifying possible future emissions of CO_2 and CH_4 from permafrost terrain, especially in identifying our proximity to the time when the permafrost regions will be a net source of atmospheric carbon, now occupies an extensive literature and research effort [3, 7]. The maps accompanying this paper indicate significant improvements to databases concerning several aspects of the permafrost environment and our computational capacity to manage and process such data. A wide-ranging set of new maps is presented in the *Arctic Permafrost Atlas* [8].

The environmental sciences use universal principles, assigning their relative importance under local or regional conditions. In the permafrost regions, geographical context is particularly important for understanding the occurrence of ground ice because the physical composition of an area is the result of history and contingency [9]. The relative emphasis on regional or configurational considerations may depend on the scale of a research question, with variation in physical conditions considered less as the area of application or simplicity of the system increases [10, 11]. Engineering projects are bound by configurational conditions because their investments are at specific locations, whereas global-scale projections are fundamentally rules-based. In between these scales lie the landscape and regional domains, where rules-based approaches have been shown to come up short in their projection of geocryological conditions because historical conditioning of the environment is commonly spatially variable [5]. Attention to regional factors has been emphasized in this paper, because that is the scale of most applications of permafrost science.

The emphasis here on permafrost warming and thaw does not include all the significant developments in permafrost science and engineering throughout 2019–2024. For instance, there has been material progress in modeling convection and its role in establishing and maintaining permafrost in blocky materials well outside the environments normally associated with perennially frozen ground [12]. Nevertheless, climate change has clearly been the primary stimulus for most current research. This review identifies two or three key developments in each of 18 subfields of permafrost science and engineering that have been recognized in the last 5 years. The comments are by researchers active in these areas; they are not as comprehensive as the reviews published as the *Transactions of the IPA* [13, 14]. This paper is presented in six thematic sections, representing (1) permafrost state, (2) physical instability, (3) the consequences of thaw for infrastructure design and (4) for biogeochemical processes, (5) research techniques, and (6) a regional initiative in the Himalayas, where baseline permafrost conditions are poorly known.

2 | State

Continuous monitoring of ground temperature and active-layer thickness (ALT) provides a time series indicating the response of permafrost terrain to climate change, but adjustments to the landscape, especially the development of landforms that result from thaw, represent the effects of climate change on permafrost to most observers [5]. The time series of temperature and thaw depth collected throughout the permafrost realm indicate the global scale of the response to climate warming, as the temperature of near-surface permafrost is increasing throughout its domain [1]. At present, one focus of permafrost modeling is to reproduce the range of ground thermal regimes at a global scale. The models are sensitive to configurational effects such as the distribution of ice in near-surface permafrost, so there has been considerable effort to provide and justify representations of the vertical and spatial distribution of ground ice. Global- or continental-scale simulations of terrestrial ground thermal regimes, and hence permafrost extent, have characteristically been based on climate simulations moderated by microclimatic factors. For subsea permafrost; however, the "climate" is remarkably uniform on the sea floor away from estuaries and river deltas, so effects associated with sea-level history assume significance for its distribution. Mapping permafrost in the Arctic continental shelves remains a priority.

2.1 | Ground Temperature Series (*Sharon Smith*)

The ground thermal regime of permafrost has been monitored at many locations in the circumpolar regions, at some sites for more than four decades [1]. Permafrost is defined in terms of

temperature, so temperature measurements are fundamental to the appraisal of the state of perennially frozen ground. Long-term records of ground temperature at or below the depth of zero annual amplitude indicate the change in permafrost thermal state. Ground temperature and its associated geotechnical properties, such as creep behavior, are keys to apprehending the response of permafrost to climate change.

In northern Canada, permafrost warming has been observed since the 1980s (Figure 1). Mean annual ground temperatures have increased by up to 0.3°C decade^{-1} in "warm" permafrost of the discontinuous permafrost zone where this index is > −2°C and by up to 1°C decade^{-1} or more in the colder continuous permafrost of the Arctic [15]. Similar rates of warming have been observed in Alaska, the Nordic regions, and Russia [16]. The rising ground temperatures are consistent with trends in air temperature, including short periods of warming or cooling imposed on the longer term trajectory. The increase in ground temperature of more than 1°C since the 1980s means that the overall range in permafrost temperatures for the circum-Arctic regions has declined.

Although ground warming at the depth of zero annual amplitude has been limited in "warm" permafrost, other observations such as shallow ground temperatures, thaw depth measured relative to a fixed reference datum, ground elevation changes, and thermokarst development indicate that widespread changes to permafrost terrain have occurred in response to climate warming [5, 15]. For example, in the Mackenzie Valley, results from a network of thaw tubes indicate that annual thaw penetration has increased since the 1990s at a median rate of 80 mm decade^{-1} at over 70% of the sites [17]. Substantial surface subsidence has accompanied this loss of ice-rich ground, at a median rate of 40 mm decade^{-1}. Similar rates have been observed in Alaska [18]. These results, when combined with systematic observations of thermokarst terrain [5], can improve assessments

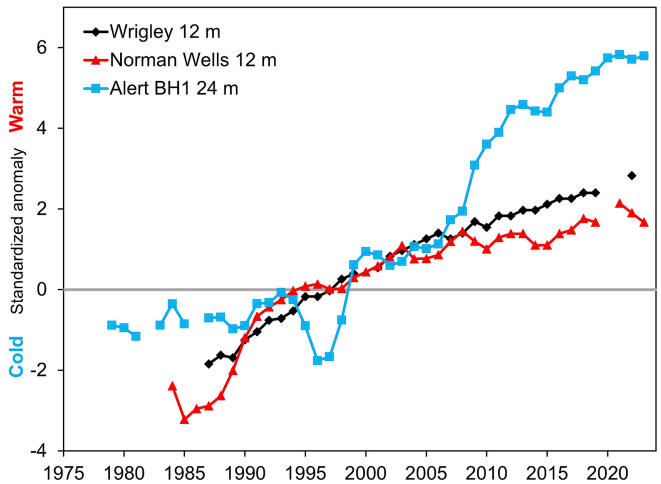

FIGURE 1 | Standardized ground temperature anomalies, relative to the 1988–2007 mean, at the depth of zero annual amplitude for sites in warm discontinuous permafrost (Norman Wells and Wrigley, NT) and the High Arctic (Alert, NU). Mean ground temperatures for 1988–2007 at the depths indicated for Wrigley, Norman Wells, and Alert were −0.8°C, −1.25°C, and −11.9°C, respectively. [Colour figure can be viewed at wileyonlinelibrary.com]

of the response of permafrost environments to a changing climate. The active layer and the near-surface permafrost immediately below are commonly the parts of permafrost terrain in which the physical consequences of climate change first appear.

2.2 | The Active Layer (*Gonçalo Vieira*)

ALT responds to climate change because the active layer's thermal regime is mainly driven by air temperature and is modified by snow accumulation. It may also be strongly influenced by diurnal insolation or changing weather in the tropical high mountains, continental Antarctica, and the High Arctic. The active layer modulates the permafrost response to surface temperatures, with its freezing and thawing controlling biophysical processes. ALT is an essential climate variable that is monitored in the Arctic, Antarctic, Qinghai-Tibet Plateau (QTP), the European Alps, and other high mountain areas. It is commonly measured with mechanical probes, thaw tubes at permanent installations, or by interpolation of ground temperatures in boreholes and, recently, has been monitored with autonomous electrical resistivity tomography (A-ERT) [19]. Low power consumption systems for A-ERT and small electrode spacings (~1 m) allow for detailed measurement of changes in active-layer state, including detection of short-lived thawing and freezing events.

In ice-rich ground, surface subsidence accompanies increasing thaw penetration [17]. ALT may remain constant, whereas subsidence continues if the thaw front reaches massive ice, such as an ice wedge, before the end of the thaw season [20]. At a hillslope site in the Canadian Beaufort Sea coast monitored for over 20 years, the mean rate of subsidence in an ice-wedge trough once the thaw front reached the massive ice was 32 mm a^{-1}, whereas in an adjacent polygon, it was 5.6 mm a^{-1} [20].

Increasing ALT has been apparent in most time series of measurements reported from the Arctic since the 1990s and from the Alaska North Slope and the Mackenzie River valley since the late 2000s [16, 21]. In cold Arctic permafrost, ALT has increased by many mm decade^{-1} and by a total of more than 100 mm in discontinuous permafrost. On the QTP, the average increase in ALT has been 196 mm decade^{-1} over the last 40 years, whereas in the European Alps, an increase of a few m has been recorded at several sites in the last 20 years [22]. The large values at the alpine sites have been observed in bedrock, whereas elsewhere, the measurements are mostly in unconsolidated material. In the Nordic Arctic (N Sweden, NE Greenland, and central Svalbard), there has been an overall increase in ALT with a significant correlation to thawing degree days in Sweden and Greenland. In Svalbard, winter temperature changes have become important, with ALT correlating inversely with freezing degree days [21]. The few long-term ALT observations from Antarctica do not show a statistically significant trend. A decrease of ALT from 2006 to 2015 in the South Shetland islands accompanied cooler summers and increased snow cover. There has been a slight increase in ALT since then. The Ross Sea region showed overall stability from 2000 to 2018, whereas slight active-layer thickening has been reported for northern Victoria Land [23]. Globally, the response of ALT to climate forcing depends on the ground ice content.

2.3 | Ground Ice (*H. Brendan O'Neill and Stephen Wolfe*)

The nature and abundance of ground ice are controlled by geologic conditions and environmental history [24]. As the ice sheets receded at the end of the last glaciation, ice wedges formed in newly exposed ground where air and ground temperatures were sufficiently low to induce repeated thermal contraction cracking. Fine-grained sediments deposited during glacial lake and marine inundation became enriched with segregated ice as permafrost established and evolved with subaerial exposure of these postglacial environments. Glacial ice, entombed within permafrost, has been preserved in high latitudes under a layer of sediment, whereas further south, this ice melted during the Holocene as climatic shifts stimulated northward advance of the tree line. Recognition of these geologic and environmental controls has been used in recent ground ice modeling across Canada [24, 25]. The mapping has contributed to renewed efforts to quantify and predict ground ice abundance at various scales in the glaciated Canadian landscape (Figure 2). In unglaciated areas, thick sequences of aggradational permafrost house large syngenetic ice wedges and segregated ice that accumulated during the Pleistocene. The distribution of these ice-rich yedoma deposits has been synthesized to produce a circum-Arctic map of this sensitive permafrost terrain, as described below (Figure 3) [26].

Landforms associated with ground ice, such as pingos and retrogressive thaw slumps, are readily observed on the ground and in satellite imagery. As a result, inventories of these features are available at regional or even circum-Arctic scales [27]. In contrast, gradual melt causing subtle subsidence may only be apparent from long-term measurements or high-precision topographic surveys. Long-term (1991–2018) records from western Canada demonstrate that subsidence is now nearly ubiquitous in sedimentary terrain across the permafrost zones because of the widespread distribution and melt of near-surface segregated ice and persistent climate warming

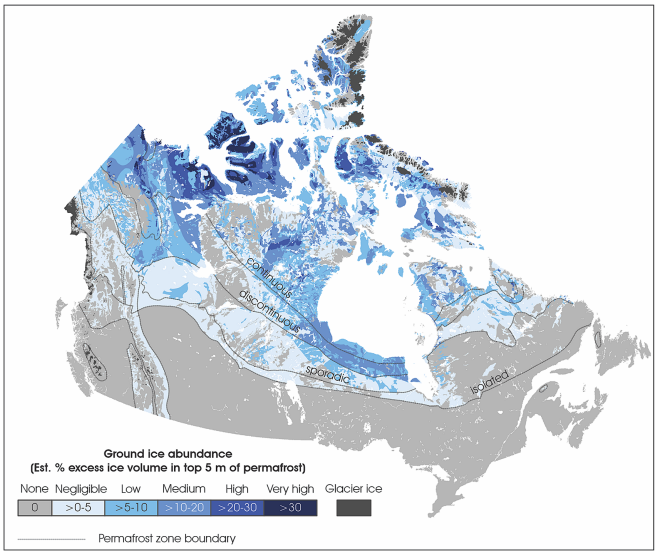

FIGURE 2 | The Ground Ice Map of Canada, depicting modeled excess ice content in the upper 5 m of permafrost [25]. [Colour figure can be viewed at wileyonlinelibrary.com]

[17]. These data show that adjustments to ALT alone may be a poor indicator of climate change effects at sites where appreciable subsidence accompanies thaw penetration. Where the surface expression of ice wedges was previously obscured by soil movement and infilling on tundra hillslopes, increased thaw penetration since the 1990s has resulted in the visible development of troughs [20]. Subsidence rates accompanying melting of hillslope ice wedges are higher than in adjacent terrain, as described above, because meltwater discharges downslope and does not refreeze in place. Long-term release of water from segregated ice and hillslope ice-wedge melt in northwest Canada is estimated to be thousands of $m^3\,km^{-2}\,a^{-1}$, which may affect regional geomorphology, hydrology, and the carbon cycle [17], even though many of the ice wedges in this region are postglacial features and of modest size in comparison with the wedges of the Pleistocene ice complex in Beringia or yedoma.

2.4 | Yedoma (*Julian Murton*)

Yedoma refers to (1) remnant geomorphic surfaces between thermokarst terrain, and/or (2) a stratigraphic unit dating from ~60 to 13 ka BP, and/or (3) a type of permafrost deposit widespread in Beringia (Figure 4) [28]. The third meaning—now gaining wider usage—refers to ice-rich silt and/or sand penetrated by large syngenetic ice wedges and attributed to sediment aggradation with syngenetic freezing over millennia in the Late Pleistocene Stage (129–11.7 ka BP). Yedoma exemplifies one of several known ice complexes formed during the Pleistocene Epoch. The strange appearance of tall, frozen cliffs exposing ground ice and frozen soil—some containing frozen carcasses of extinct mammals—mystified early explorers and scientists in Siberia and Alaska [29]. The ice was interpreted as buried, intrusive, or wedge ice, but the soil was often ignored.

The geographical distribution of terrestrial yedoma has become increasingly known, particularly through a digital circum-Arctic map and geospatial database (Figure 3) [26]. The map distinguishes between the "yedoma domain," the region outlining the maximum extent of yedoma deposits in the Late Pleistocene but where they are now interspersed with other landscape units such as drained lake basins and river valleys, and the area still underlain by yedoma. These areas are ~2,587,000 and ~480,000 km^2, respectively (Figure 3). Geographically, 81% of the terrestrial yedoma area is in northern Asia and the balance is in North America (mostly Alaska). The area of subsea yedoma is unknown. Yedoma thickness ranges from 5 to 50 m, with a mean of 17 m. Yedoma was widely distributed across Beringia during the Late Pleistocene but has been much degraded by regional erosional processes like thermokarst activity during the glacial–interglacial transition and throughout the Holocene, producing a distribution that is now fragmented.

Paleoenvironmental analyses of yedoma are developing rapidly. Some use ancient environmental DNA to indicate the former presence of animals, plants, fungi, and microbiota and thus enable reconstruction of ecosystems [30]. Ancient sedimentary DNA from silt deposited ~30–4 ka BP in central Yukon, for instance, suggests a gradual decline of grazing megafauna after

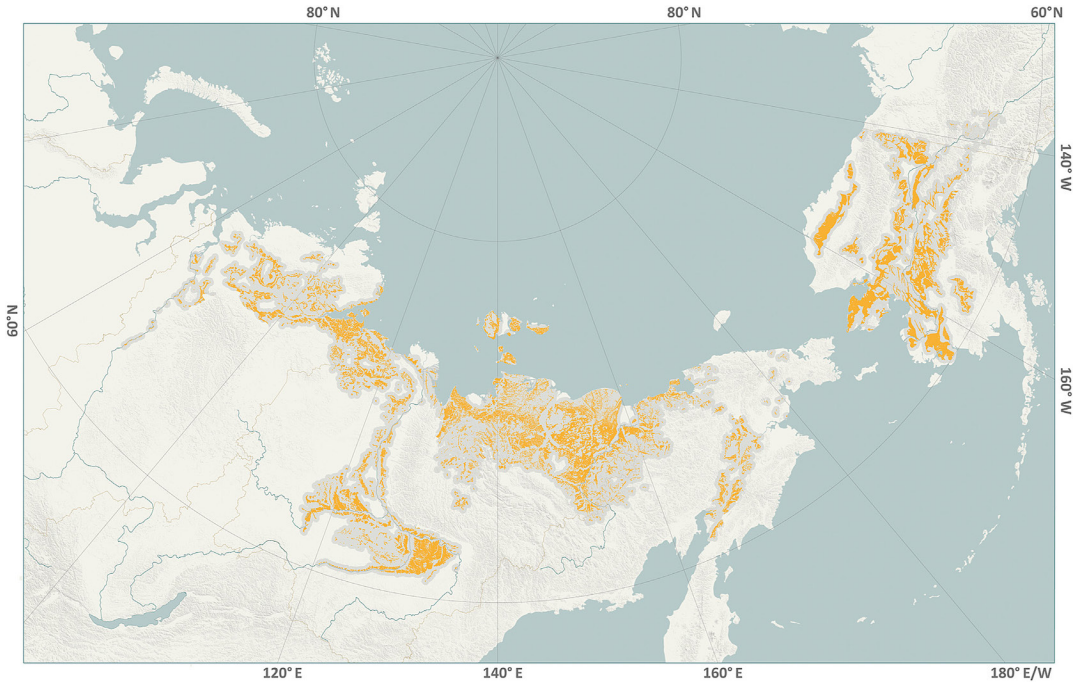

FIGURE 3 | Map of yedoma distribution in the Northern Hemisphere. Gray area denotes yedoma domain, and yellow area denotes yedoma deposits. Reproduced from [26], figure 4. [Colour figure can be viewed at wileyonlinelibrary.com]

FIGURE 4 | Syngenetic wedge ice (shiny) and yedoma silt (dark gray) that collectively comprise the Yedoma Ice Complex at the Russian stratotype of the Late Pleistocene "Yedoma Suite," Duvanny Yar, lower Kolyma River, NE Yakutia. The wedge ice melts out between columns of frozen silt, producing conical thermokarst mounds (baydzherakhs). The flattish land surface above the slump headwall is geomorphologically a yedoma surface. People for scale. Photograph by Julian Murton, 2009. [Colour figure can be viewed at wileyonlinelibrary.com]

~20 ka BP—first woolly mammoths, then steppe-bison—before a major turnover of vegetation from graminoids and forbs to woody taxa at ~13.5–10 ka BP [31]. Such replacement of Late Pleistocene mammoth–steppe by a Holocene moist dwarf-shrub ecosystem, containing sedges, birch, and willow, suggests increased ground cover and insulation, active-layer thinning, and boggy conditions. The influence of paleopermafrost environments on present ground ice conditions is now recognized as a significant factor to be accommodated in modeling the future state of permafrost.

2.5 | Modeling Climate Effects (*Sebastian Westermann*)

Knowledge of ground ice distribution is critical for predicting thaw trajectories in permafrost landscapes. Thaw of ground with excess ice triggers subsidence, alters the microtopography, and changes the small-scale interaction of ground thermal and hydrological regimes. Such thermokarst development may rapidly transform the appearance of permafrost terrain.

Classic transient permafrost models, primarily based on vertical heat conduction, use fixed grids and, consequently, are unable to simulate thermokarst processes. Recently, three-dimensional model schemes for thermokarst have been proposed, ranging from mesh-based finite-element models, with full three-dimensional treatment of heat and water fluxes [32], to tiling-based model schemes, in which energy, water, and snow are exchanged between several one-dimensional model columns or tiles. The latter concept of laterally coupled tiles has been implemented in the land components of Earth system models (ESMs) [33]. Much of this work has focused on the representation of permafrost landforms with a high ground ice content, in particular, tundra polygons and peat plateaus [34, 35].

Thermokarst simulation is highly influenced by the initial distribution of ground ice in the vertical and horizontal dimensions, which is generally prescribed from field observations. If there

is excess ice directly below the present thaw layer, even a small amount of warming may trigger its melt, leading to subsidence and, potentially, development of thermokarst. In contrast, if the ice is in deeper layers, the warming threshold for thermokarst onset is higher. Therefore, accurate initial representation of ground ice conditions is essential for reliable thermokarst simulation. This is problematic for areas with limited field observations of cryostratigraphy and, especially, for global-scale ESMs [33].

Although it may be possible to establish typical cryostratigraphies for landforms or even specific regions, numerical simulations are always subject to model-specific biases, for instance for thaw depth, and so they have the potential to misrepresent thermokarst development significantly—even if used with "true" cryostratigraphies. We may overcome this challenge by simulating not only the melting but also the development of excess ground ice, leading to a self-consistent model framework less affected by biases. In this case, the present distribution of ground ice may serve for model validation instead of defining the initial state. Although candidate models exist for segregated ice formation [36], there are currently few models designed for wedge ice accumulation, and buried glacial ice must, almost necessarily, be prescribed. Moreover, ground ice accumulation is closely linked to sedimentation and the build-up of organic carbon (OC) over millennial timescales. Therefore, a holistic understanding of permafrost landscape evolution is necessary and should guide the development of the next generation of permafrost models, even when the primary focus is on simulating climate change effects at centennial timescales. The thermal consequences of landscape history are probably easiest to estimate in the case of subsea permafrost, for which the time of inundation and the submergence sequence are key variables.

2.6 | Subsea Permafrost (*Paul Overduin*)

Our understanding of permafrost distribution in the continental shelves of the Arctic Ocean has benefited from analyses of data from the Beaufort, Kara, and Laptev seas. Legacy borehole and seismic data from the Beaufort Sea continental shelves of Canada and Alaska indicate that seismically defined subsea permafrost extends at least 3–17 km offshore from Smith Bay to Prudhoe Bay, but east of the Mackenzie Delta, it extends more than 130 km out from the coast to water up to 100 m deep [37]. In this region, the subsea permafrost is over 500 m thick near the coastline. It thins northward to the edge of the continental shelf, where the seabed subsides as ice in the sediments thaws [38].

In the Kara Sea, high-resolution seismic data, information from boreholes, and water column observations have been used to infer subsea permafrost distribution and thaw patterns. The continuous subsea permafrost approximately 400 m thick near the coast thins with increasing distance from the coastline to become discontinuous or disappear entirely beyond the 20 m isobath. Discontinuous subsea permafrost may extend further seaward out to ~110 m water depth, as in the Canadian sector. The vast East Siberian shelves, entirely exposed during the Last Glacial and with permafrost up to 700 m thick at the coastline, are likely to hold the largest province of subsea permafrost. Seismic data from the outer Laptev shelf suggest that permafrost extends northward from the coast to ~60-m water depth [39].

The available data provide an incomplete picture of the circum-Arctic distribution of subsea permafrost, its current thermal state, ice content, and susceptibility to future warming. The largest gap in our knowledge of permafrost distribution in the Arctic Ocean shelves is in the East Siberian sector and is due to very few field observations there. The variability observed beneath the Beaufort margin implies that subsea permafrost below the East Siberian shelves is also likely to vary spatially in offshore extent.

Substantial permafrost thaw, mostly due to salt diffusion, has occurred in the continental shelves over the ~21,000 years since the onset of deglaciation and consequent sea level rise. Although gas hydrates are stable over a depth interval of 100 s of meters, often entirely below the permafrost body, modeling and observations of sea-bottom temperatures show that warming of permafrost, including the effects of Arctic Amplification, may lead to a destabilization of the gas hydrate stability zone in the future [40]. However, much of the permafrost beneath the Arctic margin, and the gas hydrate stability zone associated with it, are likely to survive for millennia, even under continued climate warming [41].

3 | Physical Instability

Warming and thawing of ice-rich terrain leads to the primary geotechnical consequences of surface subsidence and instability on slopes [6, 17]. The physical stability of permafrost decreases as its temperature rises, pore ice thaws, and massive icy bodies approach their melting point. In the past, terrain instability was observed in permafrost regions after disturbances, the most widespread being forest fires [42, 43]. Now, the combined effects of climate change and disturbance, leading to thermokarst development, can be seen at an unprecedented spatial density [44]. There are few places with geomorphic evidence suggesting a previous episode of similarly rapid thermokarst development during the Holocene. In some regions, the most sensitive terrain is now understood to be underlain by relict glacial ice [45], a remarkable change from the intellectual context of the 1980s and 1990s, when segregation-intrusion was emphasized in the research on massive icy beds [46]. In mountain permafrost terrain, rock glaciers are the most prominent physical features with temperature-sensitive behavior.

3.1 | Rock Glacier Kinematics (*Isabelle Gärtner-Roer*)

Rock glaciers are lobate mountain landforms with steep frontal and lateral margins and a surface topography of ridges and furrows (Figure 5). The morphology results from creep of frozen rock debris, typically through a combination of internal deformation and shearing at depth [47]. Rock glaciers are morphological indicators of the current and former occurrence of permafrost in cold mountains around the globe.

FIGURE 5 | Rock glaciers in the Hungerlitelli, Switzerland. Photograph by Isabelle Gärtner-Roer, 2022. [Colour figure can be viewed at wileyonlinelibrary.com]

Increasing interest in mapping and monitoring rock glaciers in a standardized way led to the 2018–2023 IPA Action Group *Rock glacier inventories and kinematics*. This Action Group developed a long-term structure to coordinate compilation and dissemination of standardized rock glacier inventories and rock glacier velocity products [47]. Typical rock glacier velocities range from mm a^{-1} to several m a^{-1} with characteristic spatiotemporal changes, such as seasonal rhythms, as determined by in situ measurements and remote sensing methods. During the last three decades, combined analysis of ground temperatures, internal structures (ice, debris, and water content), and kinematics has improved process understanding and allowed the sensitivity of rock glaciers to atmospheric changes to be assessed. Although rock glacier velocity in general relates to climatic, topographic, and internal factors, its temporal variation is sensitive to changes in climatic boundary conditions, especially air temperature and snow cover [48]. These relations have been investigated for many different rock glaciers in the European Alps [49]. There are only a few long-term series of rock glacier velocities from other parts of the world [50]. Nevertheless, in 2022, *Rock Glacier Velocity*, defined as a time series of annualized surface velocities of a rock glacier unit or parts thereof, was approved as a component of the essential climate variable (ECV) *Permafrost* of the Global Climate Observing System.

In the same year, the rock glaciers of the Engadine, Switzerland, were acknowledged by the International Union of Geological Sciences, through its International Commission on Geoheritage, as one of the first 100 geological heritage sites (see https://iugs-geoheritage.org/geoheritage_sites/rockglaciers-of-the-engadine/). The award was motivated by the long history of rock glacier research and monitoring in this region, starting with the early measurements on rock glacier movement in 1923. Methods, strategies, and other experiences from this area have been shared and successfully transferred to other regions. The award applies not only to this region but also to the rock glacier research community in general, whose interests are allied with those considering hazardous events in mountain environments.

3.2 | Mass Movements (*Kjersti Gisnås and Regula Frauenfelder*)

During the past two decades, a growing number of slope failures have been reported from permafrost regions worldwide [51]. Rapid permafrost degradation has been associated with these events, because it alters the geotechnical properties of slope materials, leading to loss of structural integrity, heightened pore pressures, and reduced frictional resistance. The events have stimulated progress in three major areas: laboratory studies on the reaction of frozen soil and rock material to increasing temperatures and moisture content [52], field studies and modeling on the displacement and potential failure of unstable rock slopes [53], and examination of landslide response to climate change [6, 54].

Physical weathering is a precursor to instability on rock slopes and must commonly be studied in the laboratory. During laboratory tests of freezing rock, short-term volumetric expansion of water in cracks may lead over a few hours to measured stresses as high as 10 MPa, whereas long-term ice segregation causes stresses of 1 MPa over a couple of days [52]. These observations lead to the conclusion that crack propagation seems to dominate the antecedent processes that initiate rockfalls.

Investigations of several unstable rock slopes in northern Norway, classified nationally as high-risk sites, revealed a seasonal pattern of surface displacement with relatively high velocities in late winter and early spring and peak movement in June [53]. These movements were likely associated with fluctuations in water pressure during snowmelt. The effects of warming and thawing of frozen rock and rock joints on the mechanical strength and deformation behavior of rock slopes have been modeled for the permafrost-affected Zugspitze in southern Germany [54]. The simulations demonstrate that slope stability declines toward a critical level because of a combination of rock-bridge destruction and warming from −4 to −0.5°C of frozen rock and ice-filled joints. The model can be applied to assess future destabilization from degrading permafrost in any rock slope, and it predicts potential slope failure within the next five decades at the Zugspitze under projected future warming [54]. Continued warming may heighten the frequency and scale of rapid landslides in permafrost regions, increasing the consequences that cascade from these events.

At a larger scale, analysis of 1389 recent rockfall events in the Mont Blanc Massif indicated a strong spatial correlation between landslide incidence and permafrost occurrence. Regional rockfall propagation mapping, combining a temperature and slope-dependent susceptibility index with run-out modeling, is helping to identify potential hazard hot-spots in the French Alps [55].

Rockfall and slope instability are commonly associated with mountain environments, but the most spatially extensive and intensive example of mass movements driven by climate change is the 60-fold rise in occurrence of retrogressive thaw slumps in the rolling terrain of Banks Island, Canada, between 1984 and 2015 [6]. Over 4000 retrogressive thaw slumps were initiated along the island's eastern margin, predominantly during four notably warm summers. These data show that ice-rich continuous

FIGURE 6 | Thaw slump WR-1 in Willow River basin of Richardson Mountains, 30 km WSW of Aklavik, NT, Canada. Photograph by Jurjen van der Sluijs, 2021. [Colour figure can be viewed at wileyonlinelibrary.com]

permafrost terrain with a thin active layer is sensitive to alterations in summer climate, even in a relatively cold Arctic environment where substantial thermokarst development was not anticipated barely a decade ago. Abundant freshly developed thaw slumps have been observed in several other areas as well (Figure 6).

3.3 | Thermokarst (*Steven Kokelj*)

Thermokarst refers to the suite of processes that produce characteristic landforms from thawing of ice-rich permafrost (Figure 6). Thaw-driven mass movement, top-down ice wedge thaw, pond formation, thaw lake expansion, rapid lake drainage, and peatland degradation are among the most recognized thermokarst processes [56, 57]. Thermokarst development has been amplified by climate warming and disturbance but is controlled by ground ice conditions and the interaction of geomorphic, hydrologic, and ecosystem factors. These influence the spatial and temporal scale of thermokarst effects and give rise to distinct landforms and terrain types [5]. For example, low-lying landscapes characterized by thermokarst lakes and lithalsas are modified by thaw lake expansion, as well as by drying and drainage of wetlands. In contrast, landscapes affected by retrogressive thaw slumps are commonly underlain by glacially conditioned ice-cored terrain, or ice-rich lacustrine and yedoma deposits. Thaw of large ice-wedge polygons and trough pond expansion is transforming tundra environments, but these landforms are largely absent from discontinuous permafrost in the boreal forest.

Mapping thermokarst landforms over large areas from remotely sensed imagery has provided an empirical basis for quantifying complexity and estimating the thaw sensitivity of landscapes. The mapping has provided new information on permafrost terrain characteristics distinct from rules-based assessments of thaw sensitivity conducted at circumpolar or national scales because it integrates regional knowledge of ground ice conditions into estimates of terrain thaw sensitivity [5, 58]. The maps contextualize field studies and model outputs and support informed planning and adaptation in an era of thaw-driven change.

Climate-driven increases in the frequency and magnitude of slope failures are of particular concern because of rapid changes and the risks posed to infrastructure and, downstream, to ecosystems [6, 59]. Acquisition of broad-scale information on thaw-driven landslides at high temporal resolution is partially being overcome by advances in remote sensing technology and high-performance computing, as described below, but regional monitoring initiatives using coarser resolution imagery have proven effective in assessing retrogressive thaw slump distributions and decadal-scale temporal patterns [6]. As climate extremes intensify and ground warming modifies the behavior of permafrost materials, slope stability is being altered and thaw-driven failures are rapidly increasing in magnitude, dynamics, and effects [44, 59]. For example, an order-of-magnitude increase between 1993 and 2020 in the occurrence density and area disturbed by thaw slumps and deep-seated failures in Mackenzie River valley, Canada, from 0.65 to 6.92 $(100\,km^2)^{-1}$ and 1.92 to 29.16 ha $(100\,km^2)^{-1}$, respectively, has been associated with climate warming and destabilization of permafrost by forest fires [44].

Local studies that examine process rates, feedback, and volumetric displacement have generated particular insight into landscape evolution and downstream consequences of thermokarst activity [59], initiating efforts to determine the geomorphic and biogeochemical consequences of thermokarst in stream systems. In western Arctic Canada, it has become apparent that sediment supplied by thaw slumps and thaw-induced landslides to stream networks is orders-of-magnitude greater than the annual ability of streams to transport materials out of lower order catchments. The analysis indicates that materials already mobilized into stream valleys will require centuries or millennia to pass through the catchments and that these systems, at an early stage in the paraglacial sediment regime, present substantial potential for further thaw-related effects [59]. Such long relaxation times contrast with the immediacy of biophysical response to accelerated erosion in coastal environments, where the ocean absorbs the sediment supply almost without constraint.

3.4 | Coastal Erosion (*Benjamin Jones and David Nielsen*)

Arctic coastal regions are sensitive to land-sea linkages owing to permafrost thaw and land subsidence, sea level rise, sea ice decline, a longer open-water period, and increases in the frequency and intensity of storms [60]. Coastal erosion has accelerated across the Arctic this century, altering the environment, and posing challenges to communities and infrastructure (Figure 7). Recent observations from 14 coastal monitoring sites indicate how changes in the Arctic System are increasing erosion rates of permafrost coasts [60]. These higher and more variable rates increase pressure on communities as they cope with changes to their surroundings and way of life. Twenty-two percent of the approximately five million people living in the northern permafrost region reside in the coastal zone [61]. The increasingly dynamic coastal system will threaten more than 30% of all settlements in the permafrost regions by 2100, with entire communities being displaced or needing relocation [60, 61]. The accelerating pace of environmental and social changes in the Arctic makes it essential that global- and local-scale predictive models of coastal erosion are developed and refined.

FIGURE 7 | Permafrost block failures near Drew Point, Beaufort Sea coast of Alaska. Block failure is driven by thermal abrasion at the base of the bluffs, leading to coastal retreat rates that may exceed 10 m a^{-1}. Photograph by Benjamin Jones, 2018. [Colour figure can be viewed at wileyonlinelibrary.com]

Simulating the interaction of all the drivers of coastal erosion is numerically challenging and computationally costly, especially at climatically relevant scales. A simple, hindcast-forecast, semiempirical model accounting for the combined effect of thermo-denudation and thermo-abrasion on permafrost coasts projected that the mean annual coastal erosion rate in the Arctic could increase by a factor of 1.8 to 2.9 by the end of the century [62]. Localized, site-specific models are also being developed to physically simulate coastal erosion, for instance, to represent the mechanics and thermo-dynamics of degrading ice-rich permafrost, forced by oceanic and atmospheric boundary conditions, at a rapidly eroding site along the Beaufort Sea coast of Alaska [63]. The continued development of location-specific models is necessary to support hazard mitigation and climate change adaptation strategies for northern coastal communities. On the other hand, bolstering circum-Arctic scale models will help better parameterize the climate–carbon cycle feedback.

Several recent studies using incubations and in situ observations have explored the fate of carbon and nutrients upon release in the water column, in the sediment, and through CO_2 release in the atmosphere [60]. A recent compilation of sediment records provides a new perspective on the origin of carbon in Arctic continental shelf sediments. Roughly half of the terrigenous OC in the Beaufort, Chukchi, East Siberian, and Laptev Sea shelves originates from degraded ice-complex deposits [64], underlining the important contribution of coastal erosion and permafrost degradation to the Arctic carbon cycle.

4 | Infrastructure

Risks to the physical stability of infrastructure pose the most immediate and direct costs of the anticipated consequences of climate change in the permafrost regions [2, 10, 65]. Climate *warming* has been the primary term used to describe anticipated and observed long-term changes in the atmosphere [66], but climate *heating* may be more useful as it covers both sensible and latent energy and so explicitly connects global thermal and hydrologic regimes. Hydrologic processes and events may occur with little warning and the damage they cause to infrastructure may require immediate attention [65, 67]. Such events will increase in frequency and magnitude as the atmosphere's moisture content rises. Engineering design of infrastructure includes water management, but the emphasis in climate change preparedness in permafrost regions has been on preventing thaw of ice-rich foundation soils [2, 68]. Transportation infrastructure and physical structures in communities and at industrial projects have been the foci of much analysis, whereas failure of waste containment structures that rely on permafrost for their function and integrity is a widely recognized risk. Outside the circumpolar regions, there is much attention to engineering on the QTP, where the effects of climate change on permafrost are as prevalent as in circumpolar regions.

4.1 | Engineering Design (*Fujun Niu*)

Recent permafrost engineering in China has focused on structural design and development of equipment to remove heat efficiently from infrastructure foundations and on maintenance techniques for existing railway and highway embankments. These priorities stem from ubiquitous concern with thaw of embankment subgrades. Lhasa is the only provincial capital in China not connected to the national expressway network and considerable preparation for construction of this last link involves the design of a 40-km-long test section of highway including land bridges across stretches of sensitive permafrost on the QTP. Cooling of the subgrade is an integral part of the roadbed design. Full-scale embankments with forced and natural ventilation in warm permafrost on the eastern edge of the QTP along the Gonghe–Yushu Expressway (GYE) have confirmed the efficacy of cooling by convection [69]. Over 4 years of monitoring, thawing rates were 175 mm a^{-1} in a crushed-rock embankment (CRE), 159 mm a^{-1} in a combined CRE and heat-induced pavement embankment, 73 mm a^{-1} in a combined ventilated slab and CRE, and 55 mm a^{-1} in a duct-ventilation embankment. The results indicated that in regions where warm permafrost is degrading, cooling methods may slow ground warming beneath infrastructure but not prevent thawing in the subgrade. As a result, land bridge construction may be necessary to prevent subgrade thaw settlement caused by permafrost degradation.

Field studies on thermopile foundations at the Huashixia Permafrost Research and Observation Station in Qinghai indicated that the thermosyphon system operated for approximately 53% of the year and reduced the mean annual ground temperature by > 0.1°C a^{-1} at depths of 5–10 m [70]. A pile with compression refrigeration powered by solar cells reduced the ground temperature at a depth of 1 m by about 5°C and by about 1.5°C at 4 m compared with the initial state when the apparatus was not in operation [71]. The reduction in temperature raised the bearing capacity of the pile by strengthening the adfreeze bond between the pile and soil and by raising the bearing capacity of the soil.

Trains on the Qinghai-Tibet Railway (QTR) still operate at a running speed of 100 km h^{-1}. Structural problems principally related to thaw settlement are most evident on the railway at bridge abutments. In 2022, investigations at 880 abutments on

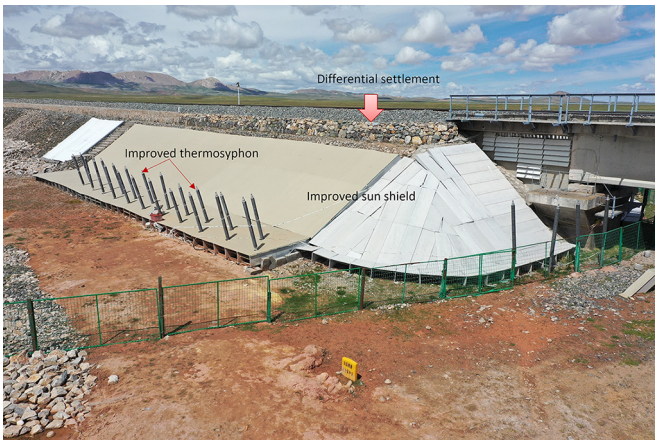

FIGURE 8 | Field installation for testing comprehensive embankment cooling measures along the QTR. Photograph by Niu Fujun, 2023. [Colour figure can be viewed at wileyonlinelibrary.com]

all 440 bridges in the permafrost sections of the QTR indicated that about 80% of the abutments were damaged by differential settlement of, on average, 153 mm [72]. Similarly, the principal structural problem on the Qinghai-Tibet Highway and GYE has been settlement due to permafrost degradation beneath and near the embankment [73]. Management of surface and supra-permafrost water has become more important for thermal stability because climate change has led to increased precipitation on the QTP. The amount of cooling now needed for embankment stability requires comprehensive measures, such as attention to embankment surfaces as well as improved thermosyphons operating beneath sun-exposed surfaces (Figure 8). Test data from the site in Figure 8 showed that after 2 years, the permafrost table in the embankment rose to 2 m above the surrounding ground, and a zone with a temperature near −2°C had appeared 2–6 m below the embankment. As thaw depths increase under roadbeds in the permafrost regions of the QTP and other areas, it may be necessary to reinforce the talik region under the embankment with physical measures as well as through enhancement of ground cooling in the freezing season. Monitoring and analysis of structural performance is one of the activities necessary to maintain the expected service life of projects built on permafrost.

4.2 | Service Life (*Ed Yarmak*)

Failure of infrastructure built on permafrost may have serious human and environmental consequences and make dramatic international news stories, as with the catastrophic failure of Tank 5 at Heat and Power Plant No. 3 in Norilsk, Russia, on 29th May 2020 [74]. The incident was widely reported as due to the warming of permafrost caused by climate change. However, the formal investigation found that the ultimate cause of failure was that the foundation of the diesel tank had not been constructed according to the original design and that warming permafrost was a subsidiary factor. Still, the specter of warming and thawing due to climate change is an ongoing concern for all long-term infrastructure on thaw-unstable permafrost.

Infrastructure founded on permafrost with near-surface excess ice will move if the climate warms, unless the design ensures subsurface warming will not reach a tipping threshold during the design life. The timing and movement will be determined by the actual construction, initial subsurface conditions, regular and emergency maintenance, and ambient climatic conditions as the structure ages. Because the climate in the Arctic is warming up to four times faster than in other areas of the world [75], the rate of climate change is of great concern to stakeholders who are living on permafrost and watching much of their world irreversibly "melt" away and their infrastructure deteriorate.

Engineers in Alaska and western Canada have access to readily available community climate charts and other tools from the University of Alaska's Scenarios Network for Alaska + Arctic Planning to project future climate in the 21st century [76]. They may use these vetted climate scenarios, without the need to become climate modelers, when designing new or rehabilitating old infrastructure.

If an engineer is commissioned to repair a structure when movement due to thaw subsidence is first detected, the work will likely be expensive because of the quantity of heat that needs to be removed from the subsurface to halt the movement. Repairs often take years to budget and plan, and by the time the physical work is initiated, the movement of the structure may be beyond acceptable limits. Further effort may then be required to keep the facility in service. Such is the experience in portions of western Alaska that are now almost permafrost-free but where permafrost was present 40 years ago. The number of variables involved in the structural response to thaw settlement makes each case unique and prevents a general solution [77, 78].

For a long service life, in addition to a conservative initial design, a regular program of monitoring, analysis, and maintenance must be undertaken by the facility owners. The thermal state of the permafrost should be assessed on a continuing basis and the owner should be prepared to perform the maintenance needed to keep the thermal state at a temperature where tolerable creep deformations will allow continued use of the infrastructure. In a warming world, almost all structures currently built on icy permafrost will become unsuitable for service at some point unless warming is halted. A design basis for structures whose service life includes thawing of permafrost in the foundation will need to be developed. Failure of built structures to perform as originally intended has become a pressing problem with respect to waste disposal at sites where permafrost was used as the confining medium.

4.3 | Waste Management (*Moritz Langer and Simone Stuenzi*)

Natural and anthropogenic contaminants have accumulated in the active layer and near-surface permafrost at circum-Arctic scale and some are currently locked in perennially frozen ground [79]. The origins and processes controlling the accumulation of such hazardous substances vary from intentional local disposal to deposition following long-range airborne or waterborne transport or portage by animals and birds. The spectrum of these contaminants ranges from inorganic elements to an array of organic substances. Persistent organic pollutants, black carbon, and heavy metals such as lead and mercury have been carried into the Arctic by atmospheric transport and have accumulated in permafrost

FIGURE 9 | Waste disposal sumps at the Mallik site, outer Mackenzie Delta, Northwest Territories. The sump in the foreground in the yellow circle is Mallik L-38, constructed in 1972. The sump in the middle distance circled in white was built in the 2000s for use by several projects [82]. Photograph by Tim Ensom, 2022. [Colour figure can be viewed at wileyonlinelibrary.com]

soils by sedimentation and after uptake by vegetation over large areas and long periods [79]. For example, the quantity of mercury accumulated in permafrost is estimated to be up to double that in nonpermafrost soils. Ground thawing will likely lead to re-emission of this mercury to the atmosphere [80].

Besides the unintentional introduction of contaminants or the formation of local pathogens in the Arctic, local deposits of municipal and industrial waste also pose environmental risks. An assessment of waste management practices in the Northwest Territories, Canada, pointed out that antifreeze chemicals and soluble heavy metal salts, often included in landfills, may not only contaminate marine environments when released but also depress the freezing point of ice-rich soil they contact and thereby accelerate permafrost thaw and dispersion into surrounding soils [81]. Industrial hazardous wastes largely comprise byproducts from drilling and mining activities, including drilling muds and fluids, heavy metals, leaked fuels, and radioactive waste.

Between 13,000 and 20,000 industrially contaminated sites are estimated in the circum-Arctic permafrost region (Figure 9) [83], and permafrost contains hazardous waste in most of them. More than 5000 of these sites will likely experience permafrost thaw this century, leading to the failure of safe disposal arrangements for toxic substances [82]. The potential for mobilization of contaminants at these sites throughout the Arctic makes identification of the sites' relative priority for practical management essential. Without such action, the contaminants may negatively affect not only local ecosystems but also the approximately 5 million people living in more than 1000 settlements on permafrost who are partly dependent on intact ecosystem services [61].

5 | Biogeochemical Effects

The surge of research interest in permafrost was driven in the 2000s by growing awareness of the carbon question and recognition of the potential effects of unstable permafrost on infrastructure. In terms of consequence to people, the direct physical effects of permafrost thaw through development of thermokarst features or erosion of the coastline are moderated by the dispersed settlements and restricted infrastructure, notwithstanding the local hazards and expense of mitigating such damage. Internationally; however, the consequences of permafrost thaw are generally associated with the emission of CO_2 and CH_4 from carbon sequestered in permafrost, the physical and geochemical aspects of an increased sediment supply, including organic matter, to rivers and the oceans, and the appearance of toxic elements in streams [84, 85]. The carbon questions have probably generated the greatest number of research publications in permafrost science during the last decade because the impacts on the atmosphere have global reach [3]. The mineralogical and ecological consequences of permafrost thaw have also been noticed, with effects that may propagate extensively [85, 86]. These effects are characteristically regional or continental in scale, well beyond the local development of thermokarst features, and may affect aquatic resources used by many people.

5.1 | Carbon Emissions (*Emma Lathrop and Ted Schuur*)

Arctic permafrost contains large stores of carbon that are vulnerable to decomposition and release as CO_2 and CH_4. These emissions represent an accelerating climate change feedback that in total is projected to be equivalent to a high-emissions nation by 2100 [3]. Nevertheless, they are underrepresented in global climate models. Multiple competing factors control the magnitude of permafrost carbon release: Warming increases microbial decomposition but may also stimulate plant growth, offsetting soil carbon losses; changing hydrology and soil moisture alter the ratio of CO_2 to CH_4 emissions; and disturbances like thaw slumps and wildfire affect carbon storage in the landscape [7]. Combining the potential net effects of these processes creates multiple future scenarios of the permafrost carbon feedback.

New estimates show that 1460–1600 Pg-C (1460–1600 billion tonnes of carbon) are stored in near-surface (0–3 m) permafrost terrain, equivalent to twice the stock of atmospheric carbon and a third of total soil OC [3]. It is held, however, in only 15% of the global area covered by soil. Deep carbon stocks and subsea permafrost are estimated to hold an additional ~1000 Pg-C. The magnitude of soil carbon relative to vegetation carbon (55 Pg-C) in permafrost landscapes suggests that increasing plant carbon uptake is not likely to offset potential losses from respiration [7].

Over the last few decades, measurement of CO_2 fluxes has shown that permafrost ecosystems have been CO_2 sinks but are now increasingly likely to become sources of this gas [87, 88]. Observed increases in plant uptake have been offset by increased respiration. In years of relatively high temperature, an increase in uptake and respiration has occurred at sites with nitrogen limitation or where summer precipitation outweighed evapotranspiration [87]. Many permafrost ecosystems have historically been CH_4 sources, and we have now quantified future changes and environmental drivers of additional CH_4 release [89]. Surface water, that is, wetlands and lakes, and soil saturation largely control CH_4 flux, regardless

of the presence of permafrost. If these surface features and wetter soils increase in area, CH_4 fluxes are expected to rise. Although CH_4 emissions represent only ~1%–12% of carbon emissions by mass [7], the higher relative forcing means CH_4 could contribute half or more of the climate feedback.

Some ice-rich landscapes are vulnerable to the development of large thermokarst features in which thaw begins soon after disturbance and from which important quantities of carbon are released (Figure 6). These features, particularly thaw slumps, are predicted to occur at points in about one quarter of the permafrost regions but may contribute up to a half of net carbon emissions [90]. In addition, increasing wildfire combusts vegetation and shallow soil carbon and exposes carbon now in permafrost to decomposition as the active layer deepens. Over time, regrowth of more abundant vegetation has the potential to offset some surface soil carbon combustion [91].

Overall, quantification of carbon stocks, flux analyses, and increasing disturbance suggest that cumulative permafrost carbon emissions will be 55 to 232 Pg-C by 2100 [3]. The most important control on this range is the permafrost region's response to anthropogenic emissions. Without mitigation, emissions from permafrost terrain may increase by 145% [3]. Greenhouse gas emissions are the most well-recognized threat to climatic stability emanating from the cryosphere. Geochemical processes may offset a modest amount of the soil biota's potential emissions, whereas geochemical contamination of the hydrosphere is a newly recognized consequence of permafrost thaw.

5.2 | Geochemical Processes (*Sophie Opfergelt and Suzanne Tank*)

Geochemical processes within permafrost landscapes affect nutrient supply, the pH of soils and freshwaters, and the broader carbon cycle. Within the carbon cycle, chemical weathering—or the dissolution of minerals by reaction with naturally occurring acids—has the capacity to affect atmospheric CO_2 at scales relevant to regional and global carbon budgets. Analysis of trends in the chemical composition of river water from large, northern rivers suggests that rates of chemical weathering have increased substantially throughout the pan-Arctic drainage basin over the past two decades [92], adding to similar findings at local and regional scales. Although a variety of factors may combine to enable this increase, permafrost thaw appears likely to be central to the change.

Two acids are primary drivers of weathering reactions. The first, carbonic acid, is produced universally by the dissolution of CO_2 in water and is transformed via weathering reactions to bicarbonate, which becomes unavailable for atmospheric exchange over millennial or longer time scales. The second, sulfuric acid, is produced locally by the oxidation of available sulfide minerals and acts on carbonate rocks to return the carbon to the contemporary carbon cycle as dissolved CO_2 and bicarbonate. Permafrost thaw has been linked to increasing sulfide oxidation in a series of tributaries of the Yukon River via increasing exposure of this rapidly weathered rock type [93]. The changing chemical composition of river water and, especially, increasing sulfide oxidation point to the need to further our understanding of the acids (sulfuric vs. carbonic) and rock types (carbonate vs. silicate) that are driving changes in weathering within permafrost terrains [92, 93].

Permafrost degradation is generating new loci and seasonal time periods for chemical weathering reactions and nutrient release. For instance, soil–water exchanges in soils with thick active layers have now been observed during late winter prior to the onset of spring thaw [94]. Increased chemical weathering releases mineral elements such as iron, aluminum, manganese, and calcium, and forms mineral surfaces such as iron oxides, thereby creating significant potential for mineral–OC interactions. Interactions of OC with mineral elements and surfaces provide physical (aggregation) or physicochemical (adsorption, complexation) protection to OC by limiting its availability for decomposition by microorganisms (Figure 10a). In addition, thermokarst-enabled changes in redox and pH within sediment can affect the stability of mineral–OC interactions involving iron [95]: Lake formation in yedoma seems to decrease the pool of iron available to protect OC, and lake drainage to increase the same iron pool (Figure 10b). In sediments displaced by retrogressive thaw slumps in ice-rich permafrost regions, more than one-third of total OC may be protected by mineral–OC interactions [96]. Importantly, the proportions of OC involved in complexation and adsorption are comparable in the sediments before and after thaw slumping, thereby illustrating that OC preservation can persist well after thaw. The occurrence and the changes in mineral–OC interactions in thaw-affected soils and sediments should be considered in the assessment of future permafrost carbon emissions, particularly from sites with changing water pathways [94–96]. Although iron is an element key to the behavior of OC liberated by thaw, other elements are also being recorded in greater concentrations than previously.

5.3 | Metal and Metalloid Mobilization (*Christine Olson, Kevin Schaefer, and Elliott Skierszkan*)

Many metals and metalloids, such as copper, iron, molybdenum, selenium, and zinc, are essential micronutrients at trace (ng/L to μg/L) concentrations but toxic at excessive exposure. Others, like arsenic, mercury, lead, and uranium, are hazardous at any level of exposure. In the last 5 years, changes in hydrology and biogeochemical reactions from permafrost thaw and permafrost carbon degradation have been linked to enhanced metal(loid) mobilization.

Mercury mobilization from thawing permafrost has probably received the most attention because of its biomagnification in Arctic wildlife and the potential exposure of Indigenous populations to cumulatively toxic levels. The mercury mass stored in the upper 3 m of permafrost exceeds the total amount of mercury stored in all other soils worldwide [97]. Its retention in soil is modulated by organic matter content, vegetation, and soil properties and so varies widely across and between landscapes. Permafrost degradation is expected to increase mercury fluxes to the atmosphere and Arctic waterways [80], and large flushes of mercury and carbon have been recorded in Arctic rivers during spring and summer [98]. Permafrost thaw may also

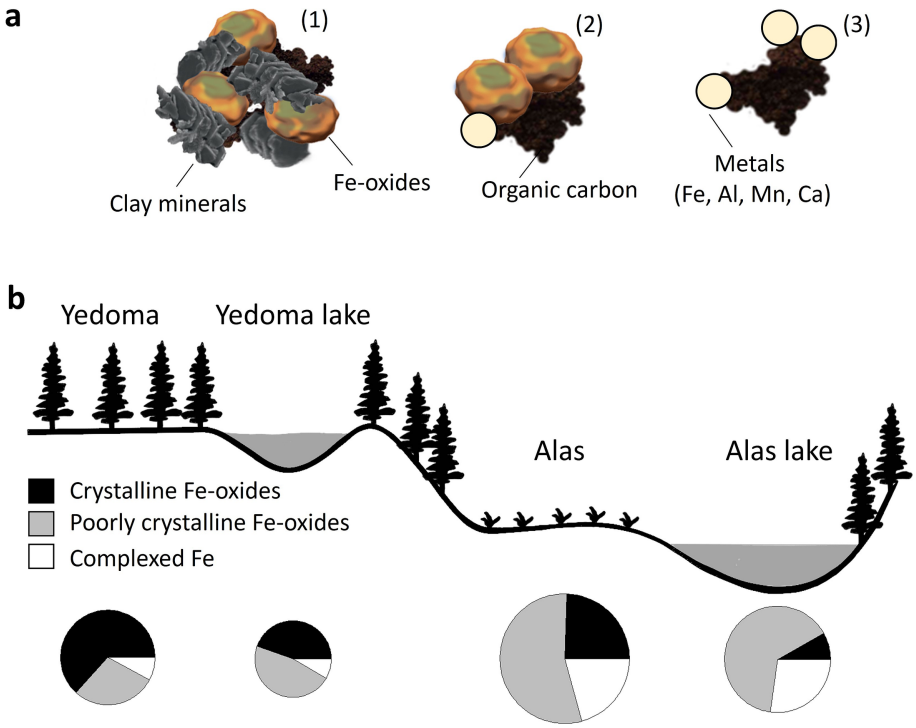

FIGURE 10 | (a) Types of mineral–organic carbon (OC) interactions contributing to OC stabilization: (1) aggregates, (2) organo–mineral associations (adsorption of OC onto mineral surfaces using cation bridge), (3) organo–metallic complexes (complexation of OC with metals). (b) Proportion of crystalline iron oxides, poorly crystalline iron oxides, and iron-complexed forms in the iron pool available to protect OC (pie chart size proportional to iron pool available to protect OC) within a sequence of permafrost degradation from Yedoma to Alas (Yukechi, Siberia, Russia; modified from [93]). [Colour figure can be viewed at wileyonlinelibrary.com]

enhance the production of methylmercury, a neurotoxicant, because of an increase in labile carbon and microbially mediated methylation hotspots in lakes, ponds, and wetlands.

Permafrost thaw may mobilize other trace metals and metalloids via processes related to enhanced OC degradation and mineral weathering. Biodegradation of thawed permafrost carbon in the active layer under water-saturated conditions creates reducing conditions that trigger release of arsenic, iron, and manganese [99, 100]. Re-oxidation of iron-(II) to iron-(III) (oxyhydr)oxides under oxic conditions has produced visually striking "rusting" of Arctic waterways [98]. The implications of changing groundwater redox conditions driven by permafrost carbon biodegradation could similarly influence the mobility of other redox-sensitive metal(loid)s, such as chromium, selenium, and uranium. Accelerated mineral weathering rates following thaw also favor breakdown of sulfide minerals and liberation of sulfuric acid. This process is acidifying some streams and mobilizing metals and metalloids at levels that are toxic to aquatic ecosystems [86]. In addition, changes in hydrological flow paths resulting from thaw alter seasonal metal (loid) export dynamics. Enhanced discharge of groundwater can be expected to drive increased export of groundwater-associated metal (loid)s—arsenic, molybdenum, and uranium—whereas a thickening active layer favors mobilization of metal cations such as aluminum, cobalt, copper, iron, nickel, and titanium in organic–metal complexes [101].

Collectively, these results indicate major changes to trace metal and metalloid mobility due to permafrost thaw. The transient and long-term impacts of individual metals and metalloids mobilized from thawing permafrost are new areas of research that were unanticipated just a few years ago.

6 | Techniques

The development of insight in science and engineering is inseparable from advances in technique, either by application of methods established in other disciplines or by use of new sensors. The single instruments that have strengthened our observational capacity in the terrestrial environment during the last decade have been unmanned aerial vehicles (UAVs) or drones. These platforms have substantially increased the capacity of projects to examine small areas with a range of airborne sensors at high frequency. Progress has also been made recently in monitoring phase transitions with electrical resistivity tomography (ERT) in ground at temperatures close to but less than 0°C, a range in which temperatures change slowly due to exchange of latent heat [1]. Similarly, the widespread availability of satellite imagery at a scale that enables reliable detection of thermokarst landforms has made detailed regional scale mapping possible and, hence, appreciation of the geographical extent of these phenomena [5, 102].

6.1 | Geophysics (*Teddi Herring*)

Geophysical surveying is becoming more common in permafrost research, with electrical and seismic methods particularly

popular. Developments in geophysical data processing have created new possibilities for permafrost characterization. Petrophysical joint inversion (PJI) techniques enable colocated ERT and seismic refraction tomography surveys to be processed together to produce quantitative models of the volumetric fractions of ice, air, rock, and liquid water [103]. This is particularly useful where ice content is difficult to quantify at site scale. Field studies employing PJI showed good agreement between observed and modeled ice content for a range of ice-poor to ice-rich landforms, demonstrating the applicability of the method in a variety of permafrost environments in high mountains [104].

Advances in geophysical instrumentation have enabled autonomous data collection, even in harsh and remote environments. For example, a robust and energy-efficient A-ERT prototype was used to collect measurements every 6 h throughout a 2-year monitoring period in Antarctica [105]. In previous ERT monitoring projects, data have typically been collected at annual intervals. A-ERT provides temporally dense information that can be used to resolve long- and short-term changes in active layer and permafrost conditions [19]. Automated systems avoid the need for repeated site visits, which can be expensive in remote locations. Two-way satellite communication with these instruments makes it possible to retrieve data and control instrument settings remotely. A-ERT instrumentation is being tested at sites in Antarctica, Canada, Switzerland, and Kyrgyzstan. The technique is expected to contribute significantly to global permafrost monitoring efforts and may soon be proposed as a basis for a fourth component of the *Permafrost* ECV.

In 2021, the International Permafrost Association Action Group *Towards an International Database of Geoelectrical Surveys on Permafrost* was created to bring together the international permafrost geophysics community and lay the foundations for an operational database of geoelectrical surveys collected in permafrost environments (https://www.unifr.ch/geo/cryosphere/en/projects/permafrost-monitoring-and-dynamics/idgsp.html). The database currently contains information from 405 ERT surveys collected between 2002 and 2023. Protocols for optimized data collection and processing are being developed to support consistent survey repetition and analysis [106]. The Action Group promotes repetition of historical ERT surveys so that detected changes can be interpreted within the context of climate warming, providing a valuable addition to traditional temperature and ALT monitoring networks. A-ERT is among the most promising developments in tools for subsurface investigation. At the ground surface, the availability of drones to carry various sensors and improvements in resolution of available remote sensing imagery and in processing capacity and techniques have had a remarkable effect on the physical scale of reliable change detection.

6.2 | Surveying With Aerial Drones (*Jurjen van der Sluijs*)

Within the last decade, aerial drones, or UAVs, have become important tools for field-based studies of permafrost, because they facilitate the acquisition of project-specific oblique and vertical aerial photographs, video footage, and various types of terrain data. Drones may carry a range of on-board sensors, for visible and thermal wavelengths, multispectral and hyperspectral applications, and Light Detection and Ranging (LiDAR) surveying. The imagery is usually transformed into ortho-mosaics and Digital elevation models using structure-from-motion photogrammetry, enabling data analysis based on geomorphological interpretation, automated image classification, and change detection methods [35, 59, 107, 108]. Drones have versatile "on-demand" deployment capabilities enabling sufficiently frequent data acquisition to capture the dynamics of permafrost landscapes that other remote monitoring systems do not regularly provide [44, 57, 59]. For example, problems for infrastructure related to permafrost may appear suddenly at specific sites (Figure 11). Data acquired by drones may also be used to reconstruct landscape features in three dimensions at high spatial resolution and reveal the development of the features over short time periods.

The characterization of topographic and elevation change, using point measurements or linear cross sections, has been an important component of research in permafrost and periglacial geomorphology [17, 20, 109]. The main contribution of drones to permafrost science and engineering is the capacity to provide three-dimensional characterization of entire permafrost landforms and their deformation that is difficult or hazardous to acquire in the field. For instance, quantification of headwall-retreat rates and sediment yield at retrogressive thaw slumps [59, 107, 108], rock glacier creep rates [110], and topographic changes in thawing peat plateaus [35]. These data help parameterize and constrain biogeochemical investigations [96] and offer calibration and validation datasets for large-area land surface models or regional monitoring [35, 58, 59].

FIGURE 11 | Inset from a three-dimensional fly-through video (Supporting S1) of a photogrammetric survey by drone, capturing retrogressive thaw slumps at NT km 28.5, Dempster Highway, Canada. The video shows the position of the slump with respect to the highway, the potential threat that downslope debris flows pose to the highway, the debris that has infilled the valley, and how the main slump has caused multiple secondary slumps by undercutting the opposing slope. Photograph and video by Jurjen van der Sluijs, 2022. [Colour figure can be viewed at wileyonlinelibrary.com]

Drone use is normally restricted to visual line-of-sight operations that limit data capture to less than about 5 km^2; however, recent technological and regulatory advances enable more extensive drone operations that may support regional-scale investigations [111]. In addition, recent advances in hardware technology allow drones to host new sensors, such as CH_4 detection equipment. Methodological improvements in software allow the integration of drone-derived and other geophysical data, for example, from ground penetrating radar or ERT [107] and developments with respect to data precision facilitate the separation of topographic changes from noise [109]. The conventional limits of remote sensing-based monitoring techniques are being superseded, thereby expanding the applications available to the permafrost community.

6.3 | Satellite Remote Sensing (*Annett Bartsch*)

Remote sensing from space has provided key information about the spatial extent of a range of landscape responses to permafrost thaw. Trends from numerical modeling results using land surface temperature agree with changes to features observable in aggregate from space [112]. Time series of satellite imagery beginning in the 1980s and 1990s, although of relatively low spatial resolution, indicate widespread and accelerating permafrost thaw across Arctic lowland areas and in high mountains. Incremental changes over large areas can now be tracked through archives of satellite imagery, especially those that span the last 20 years. At circumpolar scale, MODIS imagery has been used to detect a net loss of surface water associated with changes in size of thaw lakes during this period, including abrupt drainage, despite difficulties appearing at regional scale [113–115]. Inventories of surficial features associated with permafrost degradation have become available at regional scale across the Arctic, for instance through the automated detection of widespread retrogressive thaw slump occurrence, with > 50,000 slumps documented across central and eastern of Siberia alone [102]. Such automated techniques offer the prospect of rapid detection of environmental changes at landscape, regional, or continental scale.

Higher resolution data are becoming more available enhancing the capacity to detect physically significant changes in mountains and lowland areas. In particular, the Copernicus program of Sentinel-1 and -2 satellites, launched from 2015 onwards, has provided novel datasets at an unprecedented 10-m nominal spatial resolution and generous spatial coverage under a free data access policy. This resolution, compared with 30 m or so in previous publicly available datasets, enables the identification of settlements and infrastructure at risk from permafrost thaw and of permafrost disturbances at high precision, facilitated using AI [116]. Machine learning techniques are now commonly applied to exploit the capabilities of large datasets. Very high spatial resolution (1- and 2-m resolution) commercial datasets have been conditionally made available for permafrost research, allowing retrieval of features such as polygonal networks over an unprecedented spatial extent of the polar regions [117]. Such consistent, high-resolution data are needed for automated monitoring of changes in lowland permafrost at circumpolar scale. The ArcticDEM derived from optical stereo images at 2-m resolution for elevation has been of great general utility and will be a long-term asset for many investigations [118].

Finally, remote-sensing data have enabled the mapping of rock glacier distribution as well as the analysis of rock glacier activity worldwide [119]. InSAR techniques have been applied to determine the kinematics of over 3600 features and complement monitoring with other remote sensing techniques such as

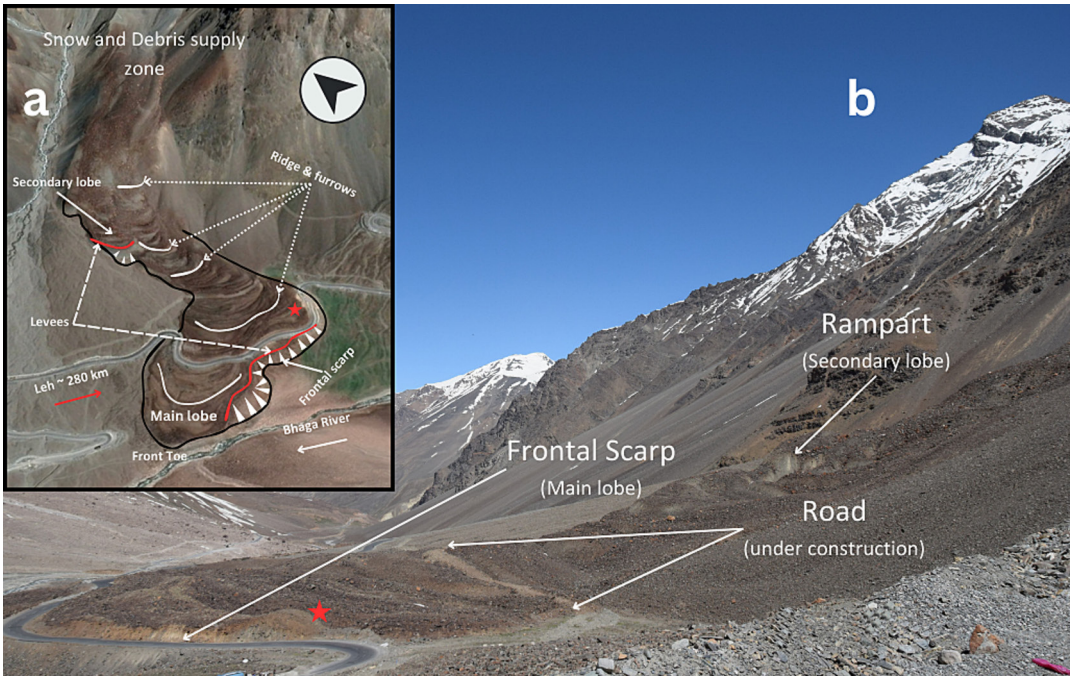

FIGURE 12 | Active rock glacier in the western Himalayas near Baralacha La, Himachal Pradesh, India. (a) Annotated view over the rock glacier with an image from Google Earth, August 22, 2022; (b) Photograph by Milap Chand Sharma, 2018. The location marked by a red star is ~4470 m asl. [Colour figure can be viewed at wileyonlinelibrary.com]

structure from motion [49, 110]. This demonstrates how Earth Observation techniques provide information required by GTN-P for continuing assessment of changes in mountain permafrost environments due to climate warming.

7 | The Himalayas

The Himalayas are probably the largest geological unit on Earth where the distribution, temperature, and ground ice characteristics of permafrost are poorly known. These mountains form a major region where the effects of climate heating have become evident in the cryosphere, but fundamental research is still necessary to establish baseline permafrost conditions and to identify the key configurational aspects controlling permafrost dynamics there. Such knowledge is critical for managing the water resources required by the growing population. Furthermore, similar natural hazards due to thawing permafrost are anticipated in the Himalayas as in other mountains. Characterization of baseline permafrost conditions is the first step in managing the risks posed by permafrost thaw. Most practical applications of permafrost science and engineering are at the regional or landscape scale, and most policy is developed and applied in this domain. The IPA Action Group *Himalayan Permafrost Consortium* aims to develop a permafrost distribution model using RS-GIS and publish the first large-scale (1:2500) permafrost map of Lahaul and Spiti District, Himachal Pradesh.

7.1 | Regional Investigation (*Soumik Das and Elora Chakraborty*)

Research on permafrost has become important in the Himalayas because perennially frozen ground facilitates major sources of freshwater for the local population [120]. The extensive permafrost in these mountains has an estimated $52 \pm 10\,km^3$ of stored water [121]. Research has concentrated upon assessing permafrost distribution, physical properties, and the potential consequences of its thaw [122]. The rugged, inaccessible, high-altitude topography of the region has often acted as a physical barrier to systematic field investigations, making remote sensing more important for mapping and terrain analysis than in other environments [123, 124].

A one-dimensional heat conduction model (GEOtop 2.0) with ground truthing at 24 sites has indicated the presence of permafrost at and above ~4900 m asl in the cold, arid Ganglass catchment of the Trans-Himalayan Ladakh region [121]. The ALT in the subwatershed varies between 0.1 and 4.2 m, whereas the mean annual ground surface temperature ranges from −10 to −0.85°C. Investigations with numerical modeling concluded that ~59% of the western Indian Himalayas are underlain by continuous and discontinuous permafrost [123].

Rock glaciers have been found to be much more resilient to climate change than glaciers in the high mountains and are key to sustainable water management in the region [120, 121]. Several rock glacier inventories for the Himalayas have been prepared since 2019, with over 3080 intact rock glaciers identified, classified, and categorized in the semiarid NW Himalayas (Figure 12). An empirical formula derived from rock glacier geometry and thickness has been used to estimate the volume of these features and their corresponding water volume equivalent [120].

Sustained positive temperature anomalies and reduced winter precipitation result in permafrost degradation, affecting socioeconomic activities and the population's livelihood [120, 121, 123]. Thawing permafrost coupled with anomalous precipitation is projected to increase mass movements such as debris flows during the postmonsoon season (July–September) in the western Himalayas [122, 123].

8 | Summary

1. Ground temperatures and ALT have increased throughout the permafrost regions accompanied by widespread thaw subsidence in ice-rich terrain [1, 17]. Subsidence has been observed at the offshore margins of subsea permafrost, which is also thawing [38].
2. A-ERT can be used to monitor phase transitions in warm permafrost, where net accumulation of energy leads to melting of ice but little ground warming [105].
3. The role of ground ice in conditioning the evolution of permafrost thermal regimes has been recognized [36], and so new ground ice maps have immediate application. Direct mapping of features derived from permafrost thaw and ground ice maps from rules-based simulations demonstrate the primacy, at present, of empirical assessments of ground ice conditions at regional scale [5].
4. Thermokarst landform dynamics have increased because of the thermal and hydrologic characteristics of climate heating combined with the effects of disturbances, particularly wildfire, that have been enhanced by the new climate conditions [44, 45]. Similarly, coastal erosion is enhanced by both a longer open-water season and enhanced fetch with reduced sea ice extent [60, 62].
5. Thaw slumps, the largest and most abundant features associated with permafrost degradation, can be identified throughout the circumpolar regions by fine-scale satellite data and machine learning techniques [102]. Initiation of these features in a High Arctic environment has been clearly associated with individual warm summers [6]. The volumes of sediment mobilized by large slumps are orders-of-magnitude higher than the carrying capacity of streams, so the physical effects of slump development will remain for centuries [59].
6. The abundant OC in some thaw slump sediments, especially features developed in yedoma, forms points of relatively intense, immediate greenhouse gas release [90]. However, the long-term geochemical effects of sediment released by these features include immobilization of OC on particle surfaces and sequestration in the muddy tongues that issue from the thawing permafrost in the slump headwalls [95].
7. Net greenhouse gas release (CO_2 and CH_4) that is widespread across sedimentary landscape units is the principal anticipated global consequence of permafrost thaw

[3, 7]. At present, the permafrost realm's carbon budget is close to balance, but every indicator implies that within two decades, the circumpolar landscape will be a net source of carbon gases, perhaps becoming equivalent to a major industrial country by the end of the century [3, 87, 89].

8. Rock glacier movement has accelerated in the European Alps, at least, and is attributed to climate forcing [49]. Detection of these fine movements is possible because of the availability of high-resolution imagery and development in data processing techniques [117]. *Rock glacier velocity* is now a formal index of changing permafrost conditions.
9. Rockfall and other slope failures from permafrost thaw are the immediate hazards affecting infrastructure corridors and communities in high mountain regions [51]. Management of risk posed by these processes, especially in developing countries, will need detailed mapping and land use zoning [55].
10. Slope instability due to thawing permafrost is recognized in the Himalayas, but failing natural water supplies are more immediate and constant concerns [120, 121].
11. Engineering design recognizes that permafrost will thaw beneath most new structures over their intended service life [78]. Comprehensive testing of multiple approaches to maintaining frozen ground has demonstrated several techniques that reduce rates of thaw beneath structures [69–71] but has not suggested it can be eliminated.
12. Permafrost was the design containment medium at thousands of disposal sites for industrial hazardous waste. Conditions are now ripe for failure at many of these sites [83].
13. Thawing of permafrost has released trace elements, some toxic, into ground and surface waters [98, 100]. Some of these have been deposited after atmospheric transport from industrial regions [80], but others come from bedrock, soil, and sediments [100].

9 | Conclusion

Geocryology has become the science of an environment that is responsive to climate change. Many of the effects regarding permafrost that have been observed or projected are unwelcome in communities and for infrastructure but are nevertheless inevitable because atmospheric concentration of CO_2 is now above Pleistocene levels, it is not possible to reverse emissions, and sequestration in ocean sediments is orders-of-magnitude slower than anthropogenic production of greenhouse gases [125]. Projection of effects from permafrost thaw, like accelerated coastal erosion, net emission of greenhouse gases, hillslope failures, widespread subsidence, and discharge of contaminants can assist in managing the timescale, location, and intensity of events and processes. However, empirical evidence of change appears to be more persuasive with the public and decision makers than theoretical projection onto the future, reinforcing the need for continued observation and monitoring. Permafrost, even thin near-surface permafrost on the order of 10 m thick near its southern margins, will be with us for millennia because the rate of thaw declines with depth [126]. Eradication of permafrost has been reported, however, in wetlands, where convective heat transport is enhanced and saturated conditions in high-porosity organic soils may retard refreezing of thawed ground [127].

Most of the topics discussed in this paper are amenable to monitoring. Some have long-term programs that have continued for several decades, such as for ground temperatures, and others, such as contaminants released from thawing permafrost, are relatively new considerations. Some concern discrete features, such as thaw slumps, and others involve landscape-scale change, as with thaw subsidence. Some require advanced machine learning techniques, such as detection of surface disturbances at circumpolar scale, and others, such as active layer probing, do not. Nevertheless, long-term monitoring programs to detect significant changes in the environment will only be effective if data collection is accompanied by the requisite analysis and clearly defined research questions are addressed.

The occurrence and distribution of ground ice are critical to many of the topics considered above. Rates of thaw penetration, for example, are important for projecting carbon emissions and depend on near-surface ice content, so configurational aspects, particularly site history, will always need to be understood. However, there has been only limited success in quantitative modeling of ground ice in the landscape that has led to predictive confidence [128, 129]. This and the inaccessibility of Russian landscapes for field studies and communication with our colleagues there are possibly the most significant problems currently facing the permafrost research community.

Acknowledgments

The authors of this paper acknowledge the numerous agencies that have supported the research described and with gratitude the careful review and editorial suggestions of A.G. Lewkowicz that led to many improvements in the text. Carleton University and the International Permafrost Association have supported dissemination of the paper. In 1983, the founders of the association envisioned that collaboration toward the development of permafrost science and engineering would be best stimulated by holding periodic international conferences and by commissioning reviews to take stock of the field, identify key innovations, and point to ways forward [130]. We are grateful for their vision.

Data Availability Statement

Data sharing is not applicable to this article as no datasets were generated or analyzed during the current study.

References

1. S. L. Smith, H. B. O'Neill, K. Isaksen, J. Noetzli, and V. E. Romanovsky, "The Changing Thermal State of Permafrost," *Nature Reviews Earth and Environment* 3, no. 1 (2022): 10–23, https://doi.org/10.1038/s43017-021-00240-1.

2. J. Hjort, D. Streletskiy, G. Doré, Q. Wu, K. Bjella, and M. Luoto, "Impacts of Permafrost Degradation on Infrastructure," *Nature Reviews Earth and Environment* 3, no. 1 (2022): 24–38, https://doi.org/10.1038/s43017-021-00247-8.

3. E. A. G. Schuur, B. W. Abbott, R. Commane, et al., "Permafrost and Climate Change: Carbon Cycle Feedbacks From the Warming Arctic," *Annual Review of Environment and Resources* 47 (2022): 343–371, https://doi.org/10.1146/annurev-environ-012220-011847.

4. C. R. Burn, "The Periglacial Environment. Fourth Edition. By Hugh M. French. 2018. John Wiley & Sons. Chichester, UK, and Joboken, New Jersey," *Permafrost and Periglacial Processes* 30, no. 3 (2019): 239–241, https://doi.org/10.1002/ppp.2009.

5. S. V. Kokelj, T. Gringras-Hill, S. V. Daly, et al., "The Northwest Territories Thermokarst Mapping Collective: A Northern-Driven Mapping Collaborative Toward Understanding the Effects of Permafrost Thaw," *Arctic Science* 9, no. 4 (2023): 886–918, https://doi.org/10.1139/AS-2023-0009.

6. A. G. Lewkowicz and R. G. Way, "Extremes of Summer Climate Trigger Thousands of Thermokarst Landslides in a High Arctic Environment," *Nature Communications* 10, no. 4 (2019): 1329, https://doi.org/10.1038/s41467-019-09314-7.

7. C. C. Treat, A.-M. Virkkala, E. Burke, et al., "Permafrost Carbon: Progress Understanding Controls, Stocks, and Fluxes Across Terrestrial Ecosystems in the Pan-Arctic Region," *Journal of Geophysical Research: Biogeosciences* 129, no. 3 (2024): e2023JG007638, https://doi.org/10.1029/2023JG007638.

8. L. Westerveld, T. Kurvits, T. Schoolmeester, et al., *Arctic Permafrost Atlas* (Arendal, Norway: GRID-Arendal, 2023), https://doi.org/10.61523/KPJI4549.

9. G. G. Simpson, "Historical Science," in *The Fabric of Geology*, ed. C. C. Albritton, Jr. (Reading, MA: Addison-Wesley, 1963): 24–48.

10. J. Hjort, O. Karjalainen, J. Aalto, et al., "Degrading Permafrost Puts Arctic Infrastructure at Risk by Mid-Century," *Nature Communications* 9, no. 12 (2018): 5147, https://doi.org/10.1038/s41467-018-07557-4.

11. J. R. Mackay, "Seasonal Growth Bands in Pingo Ice," *Canadian Journal of Earth Sciences* 27, no. 8 (1990): 1115–1125, https://doi.org/10.1139/e90-116.

12. J. Wicky, C. Hilbich, R. Delaloye, and C. Hauck, "Modeling the Link Between air Convection and the Occurrence of Short-Term Permafrost in a Low-Altitude Cold Talus Slope," *Permafrost and Periglacial Processes* 35 (2024): 202–217, https://doi.org/10.1002/ppp.2224.

13. C. R. Burn, "Transactions of the International Permafrost Association: Number 2," *Permafrost and Periglacial Processes* 27, no. 4 (2016): 323, https://doi.org/10.1002/ppp.1937.

14. C. R. Burn, "Transactions of the International Permafrost Association: Number 3," *Permafrost and Periglacial Processes* 31, no. 3 (2020): 343–345, https://doi.org/10.1002/ppp.2058.

15. S. L. Smith, C. Duchesne, and H. B. O'Neill, "Long-Term Permafrost Monitoring in Northern Canada—What Have We Learned?," in *Proceedings of the 12th International Conference on Permafrost*, eds. R. A. Beddoe and K. C. Karunaratne (Ottawa, ON: International Permafrost Association, 2024): 398–404, https://doi.org/10.52381/ICOP2024.84.1.

16. S. L. Smith, V. E. Romanovsky, K. Isaken, et al., "Permafrost," State of the Climate in 2022, Bulletin of the American Meteorological Society 104 (2023): S301–S305, https://doi.org/10.1175/BAMS-D-23-0079.1.

17. H. B. O'Neill, S. L. Smith, C. R. Burn, C. Duchesne, and Y. Zhang, "Widespread Permafrost Degradation and Thaw Subsidence in Northwest Canada," *Journal of Geophysical Research: Earth Surface* 128, no. 8 (2023): e2023JF007262, https://doi.org/10.1029/2023JF007262.

18. K. E. Nyland, N. I. Shiklomanov, D. A. Streletskiy, F. E. Nelson, A. E. Klene, and A. L. Kholodov, "Long-Term Circumpolar Active Layer Monitoring (CALM) Program Observations in Northern Alaskan Tundra," *Polar Geography* 44, no. 3 (2021): 167–185, https://doi.org/10.1080/1088937X.2021.1988000.

19. M. Farzamian, G. Vieira, F. A. Monteiro Santos, et al., "Detailed Detection of Active Layer Freeze–Thaw Dynamics Using Quasi-Continuous Electrical Resistivity Tomography (Deception Island, Antarctica)," *Cryosphere* 14, no. 3 (2020): 1105–1120, https://doi.org/10.5194/tc-14-1105-2020.

20. C. R. Burn, A. G. Lewkowicz, and M. A. Wilson, "Long-Term Field Measurements of Climate-Induced Thaw Subsidence Above Ice Wedges on Hillslopes, Western Arctic Canada," *Permafrost and Periglacial Processes* 32, no. 2 (2021): 261–276, https://doi.org/10.1002/ppp.2113.

21. S. M. Strand, H. H. Christiansen, M. Johansson, J. Åkerman, and O. Humlum, "Active Layer Thickening and Controls on Interannual Variability in the Nordic Arctic Compared to the Circum-Arctic," *Permafrost and Periglacial Processes* 32, no. 1 (2021): 47–58, https://doi.org/10.1002/ppp.2088.

22. J. Noetzli, H. H. Christiansen, F. Hrbáček, et al., "Permafrost Temperature and Active Layer Thickness," State of the Climate in 2022, *Bulletin of the American Meteorological Society* 104, no. 9 (2023): S39–S41, https://doi.org/10.1175/BAMS-D-23-0079.1.

23. F. Hrbáček, M. Oliva, C. Hansen, et al., "Active Layer and Permafrost Thermal Regimes in the Ice-Free Areas of Antarctica," *Earth Science Reviews* 242 (2023): 104458, https://doi.org/10.1016/j.earscirev.2023.104458.

24. H. B. O'Neill, S. A. Wolfe, and C. Duchesne, "New Ground Ice Maps for Canada Using a Paleogeographic Modelling Approach," *Cryosphere* 13, no. 3 (2019): 753–773, https://doi.org/10.5194/tc-13-753-2019.

25. H. B. O'Neill, S. A. Wolfe, and C. Duchesne, *Ground Ice Map of Canada (Version 1.1)* (Ottawa, ON: Geological Survey of Canada, 2023), https://doi.org/10.4095/326885.

26. J. Strauss, S. Laboor, L. Schirrmeister, et al., "Circum-Arctic Map of the Yedoma Permafrost Domain," *Frontiers in Earth Science* 9 (2021): 758360, https://doi.org/10.3389/feart.2021.758360.

27. S. A. Wolfe, P. D. Morse, R. Parker, and M. R. Phillips, "Distribution and Morphometry of Pingos, Western Canadian Arctic, Northwest Territories, Canada," *Geomorphology* 431 (2023): 108694, https://doi.org/10.1016/j.geomorph.2023.108694.

28. L. Schirrmeister, D. Froese, S. Wetterich, J. Strauss, A. Veremeeva, and G. Grosse, "Yedoma: Late Pleistocene Ice-Rich Syngenetic Permafrost of Beringia," in *Encyclopedia of Quaternary Science*, 3rd ed. S. A. Elias (Amsterdam: Elsevier, 2024), https://doi.org/10.1016/B978-0-323-99931-1.00223-3.

29. Y. Shur, D. Fortier, M. T. Jorgenson, et al., "Yedoma Permafrost Genesis: More Than 150 Years of Mystery and Controversy," *Frontiers in Earth Science* 9 (2022): 757891, https://doi.org/10.3389/feart.2021.757891.

30. J. Courtin, A. Perfumo, A. A. Andreev, et al., "Pleistocene Glacial and Interglacial Ecosystems Inferred From Ancient DNA Analyses of Permafrost Sediments From Batagay Megaslump, East Siberia," *Environmental DNA* 4, no. 6 (2022): 1265–1283, https://doi.org/10.1002/edn3.336.

31. T. J. Murchie, A. J. Monteath, M. E. Mahony, et al., "Collapse of the Mammoth-Steppe in Central Yukon as Revealed by Ancient Environmental DNA," *Nature Communications* 12, no. 12 (2021): 7120, https://doi.org/10.1038/s41467-021-27439-6.

32. S. L. Painter, E. T. Coon, A. J. Khattak, and J. D. Jastrow, "Drying of Tundra Landscapes Will Limit Subsidence-Induced Acceleration of Permafrost Thaw," *Proceedings of the National Academy of Sciences* 120, no. 8 (2023): e2212171120, https://doi.org/10.1073/pnas.221217112.

33. N. D. Smith, E. J. Burke, K. S. Aas, et al., "Explicitly Modelling Microtopography in Permafrost Landscapes in a Land Surface Model (JULES vn5. 4_microtopography)," *Geoscientific Model Development* 15, no. 9 (2022): 3603–3639, https://doi.org/10.5194/gmd-15-3603-2022.

34. J. Nitzbon, M. Langer, S. Westermann, L. Martin, K. S. Aas, and J. Boike, "Pathways of Ice-Wedge Degradation in Polygonal Tundra Under Different Hydrological Conditions," *Cryosphere* 13, no. 4 (2019): 1089–1123, https://doi.org/10.5194/tc-13-1089-2019.

35. L. C. Martin, J. Nitzbon, J. Scheer, et al., "Lateral Thermokarst Patterns in Permafrost Peat Plateaus in Northern Norway," *Cryosphere* 15, no. 7 (2021): 3423–3442, https://doi.org/10.5194/tc-15-3423-2021.

36. J. Aga, J. Boike, M. Langer, T. Ingeman-Nielsen, and S. Westermann, "Simulating Ice Segregation and Thaw Consolidation in Permafrost Environments With the CryoGrid Community Model," *Cryosphere* 17, no. 10 (2023): 4179–4206, https://doi.org/10.5194/tc-17-4179-2023.

37. H. Grob, M. Riedel, M. J. Duchesne, et al., "Revealing the Extent of Submarine Permafrost and Gas Hydrates in the Canadian Arctic Beaufort Sea Using Seismic Reflection Indicators," *Geochemistry, Geophysics, Geosystems* 24, no. 5 (2023): e2023GC010884, https://doi.org/10.1029/2023GC010884.

38. C. K. Paull, S. R. Dallimore, Y. K. Jin, and H. Melling, "Rapid Seafloor Changes Associated With the Degradation of Arctic Submarine Permafrost," *Proceedings of the National Academy of Sciences* 119, no. 12 (2022): e2119105119, https://doi.org/10.1073/pnas.2119105119.

39. V. Bogoyavlensky, A. Kishankov, A. Kazanin, and G. Kazanin, "Distribution of Permafrost and Gas Hydrates in Relation to Intensive Gas Emission in the Central Part of the Laptev Sea (Russian Arctic)," *Marine and Petroleum Geology* 138 (2022): 105527, https://doi.org/10.1016/j.marpetgeo.2022.105527.

40. Z. Li, E. Spangenberg, J. M. Schicks, and T. Kempka, "Numerical Simulation of Coastal Sub-Permafrost Gas Hydrate Formation in the Mackenzie Delta, Canadian Arctic," *Energies* 15, no. 14 (2022): 4986, https://doi.org/10.3390/en15144986.

41. V. V. Malakhova and A. V. Eliseev, "Subsea Permafrost and Associated Methane Hydrate Stability Zone: How Long Can They Survive in the Future?," *Theoretical and Applied Climatology* 155, no. 4 (2024): 3329–3346, https://doi.org/10.1007/s00704-023-04804-7.

42. J. R. Mackay, "Disturbances to the Tundra and Forest Tundra Environment of the Western Arctic," *Canadian Geotechnical Journal* 7, no. 4 (1970): 420–432, https://doi.org/10.1139/t70-05.

43. J. R. Mackay, "Active Layer Changes (1968–1993) Following the Forest-Tundra Fire Near Inuvik, N.W.T. Canada," *Arctic and Alpine Research* 27, no. 4 (1995): 323–336, https://doi.org/10.1080/00040851.1995.12003129.

44. J. M. Young, A. Alvarez, J. van der Sluijs, et al., "Recent Intensification (2004–2020) of Permafrost Mass-Wasting in the Central Mackenzie Valley Foothills Is a Legacy of Past Forest Fire Disturbances," *Geophysical Research Letters* 49, no. 24 (2022): e2022GL100559, https://doi.org/10.1029/2022GL100559.

45. S. V. Kokelj, T. C. Lantz, J. Tunnicliffe, R. Segal, and D. Lacelle, "Climate-Driven Thaw of Permafrost Preserved Glacial Landscapes, Northwestern Canada," *Geology* 45, no. 4 (2017): 371–374, https://doi.org/10.1130/G38626.1.

46. J. R. Mackay and S. R. Dallimore, "Massive Ice of the Tuktoyaktuk Area, Western Arctic Coast, Canada," *Canadian Journal of Earth Sciences* 29, no. 6 (1992): 1235–1249, https://doi.org/10.1139/e92-09.

47. RGIK, "Guidelines for Inventorying Rock Glaciers: Baseline and Practical Concepts (Version 1.0)," (2023, IPA Action Group: Rock glacier inventories and kinematics, 25), https://doi.org/10.51363/unifr.srr.2023.002.

48. A. Cicoira, J. Beutel, J. Faillettaz, I. Gärtner-Roer, and A. Vieli, "Resolving the Influence of Temperature Forcing Through Heat Conduction on Rock Glacier Dynamics: A Numerical Modelling Approach," *Cryosphere* 13, no. 3 (2019): 927–942, https://doi.org/10.5194/tc-13-927-2019.

49. A. Kellerer-Pirklbauer, X. Bodin, R. Delaloye, et al., "Acceleration and Interannual Variability of Creep Rates in Mountain Permafrost Landforms (Rock Glacier Velocities) in the European Alps in 1995–2022," *Environmental Research Letters* 19, no. 3 (2024): 034022, https://doi.org/10.1088/1748-9326/ad25a4.

50. C. Pellet, X. Bodin, D. Cusicanqui, et al., "Rock Glacier Velocity," State of the Climate in 2022, Bulletin of the American Meteorological Society 104, no. 9 (2023): S41–S42, https://doi.org/10.1175/2023BAMSStateoftheClimate.1.

51. M. Stoffel, D. G. Trappmann, M. I. Coulli, et al., "Rockfall From an Increasingly Unstable Mountain Slope Driven by Climate Warming," *Nature Geoscience* 17, no. 3 (2024): 249–254, https://doi.org/10.1038/s41561-024-01390-9.

52. D. Draebing and M. Krautblatter, "The Efficacy of Frost Weathering Processes in Alpine Rockwalls," *Geophysical Research Letters* 46, no. 12 (2019): 6516–6524, https://doi.org/10.1029/2019GL081981.

53. B. Etzelmüller, J. Czekirda, F. Magnin, et al., "Permafrost in Monitored Unstable Rock Slopes in Norway—New Insights From Rock Wall Temperature Monitoring, Geophysical Surveying and Numerical Modelling," *Earth Surface Dynamics* 10, no. 1 (2022): 1–55, https://doi.org/10.5194/esurf-10-97-2022.

54. P. Mamot, S. Weber, S. Eppinger, and M. Krautblatter, "A Temperature-Dependent Mechanical Model to Assess the Stability of Degrading Permafrost Rock Slopes," *Earth Surface Dynamics* 9, no. 5 (2021): 1125–1151, https://doi.org/10.5194/esurf-9-1125-2021.

55. M. Cathala, F. Magnin, L. Ravanel, et al., "Mapping Release and Propagation Areas of Permafrost-Related Rock Slope Failures in the French Alps: A New Methodological Approach at Regional Scale," *Geomorphology* 448 (2024): 109032, https://doi.org/10.1016/j.geomorph.2023.109032.

56. I. Nitze, S. W. Cooley, C. Duguay, B. Jones, and G. Grosse, "The Catastrophic Thermokarst Lake Drainage Events of 2018 in Northwestern Alaska: Fast-Forward Into the Future," *Cryosphere* 14, no. 12 (2020): 4279–4297, https://doi.org/10.5194/tc-14-4279-2020.

57. J. Luo, F. Niu, Z. Lin, M. Liu, G. Yin, and Z. Gao, "Inventory and Frequency of Retrogressive Thaw Slumps in Permafrost Region of the Qinghai–Tibet Plateau," *Geophysical Research Letters* 49, no. 23 (2022): e2022GL099829, https://doi.org/10.1029/2022GL099829.

58. Y. Wang, R. G. Way, J. Beer, A. Forget, R. Tutton, and M. C. Purcell, "Significant Underestimation of Peatland Permafrost Along the Labrador Sea Coastline in Northern Canada," *Cryosphere* 17, no. 1 (2023): 63–78, https://doi.org/10.5194/tc-17-63-2023.

59. S. V. Kokelj, J. Kokoszka, J. van der Sluijs, et al., "Thaw-Driven Mass Wasting Couples Slopes With Downstream Systems, and Effects Propagate Through Arctic Drainage Networks," *Cryosphere* 15, no. 7 (2021): 3059–3081, https://doi.org/10.5194/tc-15-3059-2021.

60. A. M. Irrgang, M. Bendixen, L. M. Farquharson, et al., "Drivers, Dynamics and Impacts of Changing Arctic Coasts," *Nature Reviews Earth and Environment* 3, no. 1 (2022): 39–54, https://doi.org/10.1038/s43017-021-00232-1.

61. J. Ramage, L. Jungsberg, S. Wang, S. Westermann, H. Lantuit, and T. Heleniak, "Population Living on Permafrost in the Arctic," *Population and Environment* 43, no. 1 (2021): 22–38, https://doi.org/10.1007/s11111-020-00370-6.

62. D. M. Nielsen, P. Pieper, A. Barkhordarian, et al., "Increase in Arctic Coastal Erosion and Its Sensitivity to Warming in the Twenty-First Century," *Nature Climate Change* 12, no. 3 (2022): 263–270, https://doi.org/10.1038/s41558-022-01281-0.

63. J. Frederick, A. Mota, I. Tezaur, and D. Bull, "A Thermo-Mechanical Terrestrial Model of Arctic Coastal Erosion," *Journal of Computational and Applied Mathematics* 397 (2021): 113533, https://doi.org/10.1016/j.cam.2021.113533.

64. J. Martens, B. Wild, I. Semiletov, O. V. Dudarev, and Ö. Gustafsson, "Circum-Arctic Release of Terrestrial Carbon Varies Between Regions and Sources," *Nature Communications* 13, no. 1 (2022): 5858, https://doi.org/10.1038/s41467-022-33541-0.

65. A. B. Schetselaar and C. R. Burn, "Increases in Highway Maintenance Costs in a Permafrost Environment Undergoing Climate Change, Yukon, Canada," in *Proceedings of the 12th International Conference on Permafrost*, eds. R. A. Beddoe and K. C. Karunaratne (Ottawa, ON: International Permafrost Association, 2024): 373–381, https://doi.org/10.52381/ICOP2024.82.1.

66. A. B. Schetselaar, T. S. Andersen, and C. R. Burn, "Performance of Climate Projections for Yukon and Adjacent Northwest Territories, 1991–2020," *Arctic* 76, no. 3 (2023): 244–264, https://doi.org/10.14430/arctic77263.

67. C. R. Burn, J. L. Moore, H. B. O'Neill, et al., "Permafrost Characterization of the Dempster Highway, Yukon and Northwest Territories," in *Proceedings of the 68th Canadian Geotechnical Conference and 7th Canadian Permafrost Conference*, Paper 705 (Richmond, BC: Canadian Geotechnical Society, 2015), https://carleton.ca/permafrost/wp-content/uploads/705.pdf.

68. Canadian Standards Association, *Technical Guide: Infrastructure in Permafrost: A Guideline for Climate Change Adaptation* (Toronto: Canadian Standards Association, 2019) CSA PLUS 4011:19.

69. S. Wang, Q. Zhang, Y. Dong, et al., "Full-Scale Site Evaluation of Ventilation Expressway Embankments Underlain by Warm Permafrost Along the Gonghe–Yushu Expressway," *Frontiers in Structural and Civil Engineering* 17, no. 7 (2023): 1047–1059, https://doi.org/10.1007/s11709-023-0034-6.

70. Y. Shang, F. Niu, G. Li, J. Fang, and Z. Gao, "Application of a Concrete Thermal Pile in Cooling the Warming Permafrost Under Climate Change," *Advances in Climate Change Research* 15, no. 1 (2024): 170–183, https://doi.org/10.1016/j.accre.2023.09.002.

71. Z. Sun, J. Liu, T. Hu, T. You, and J. Fang, "A Solar Compression Refrigeration Apparatus to Cool Permafrost Embankment," *Applied Thermal Engineering* 223 (2023): 120034, https://doi.org/10.1016/j.applthermaleng.2023.120034.

72. P. He, F. Niu, Y. Huang, S. Zhang, and C. Jiao, "Distress Characteristics in Embankment-Bridge Transition Section of the Qinghai-Tibet Railway in Permafrost Regions," *International Journal of Disaster Risk Science* 14 (2023): 680–696, https://doi.org/10.1007/s13753-023-00506-w.

73. Y. Huang, F. Niu, J. Chen, P. He, K. Yuan, and W. Su, "Express Highway Embankment Distress and Occurring Probability in Permafrost Regions on the Qinghai-Tibet Plateau," *Transportation Geotechnics* 42 (2023): 101069, https://doi.org/10.1016/j.trgeo.2023.101069.

74. Environmental Resources Management Limited, "Review of May 2020 Catastrophic Tank Failure," HPP-3, Norilsk, (2020), https://nornickel.com/upload/iblock/746/erm_1a_report_for_nornickel_ett_public_issued_25_11_20_en.pdf.

75. M. Rantanen, A. Y. Karpechko, A. Lipponen, et al., "The Arctic Has Warmed Nearly Four Times Faster Than the Globe Since 1979," *Communications Earth & Environment* 3 (2022): 168, https://doi.org/10.1038/s43247-022-00498-3.

76. https://snap.uaf.edu/tools/community-charts.

77. K. Bjella, H. Brooks, Z. Yang, and E. Yarmak, "Synopsis: Permafrost Engineering in a Warming Climate—Current State and Future Strategy," in *Permafrost 2021: Merging Permafrost Science and Cold Regions Engineering, Proceedings of the Regional Conference on Permafrost 2021 and the 19th International Conference on Cold Regions Engineering*, ed. J. Zufelt (Reston, VA: American Society of Civil Engineers, 2021), 233–244, https://doi.org/10.1061/9780784483589.022.

78. W. Schnabel, D. Goering, and A. Dotson, "Permafrost Engineering on Impermanent Frost," *Bridges* 50, no. 1 (2020): 16–23, https://www.nae.edu/228948/Permafrost-Engineering-on-Impermanent-Frost.

79. K. R. Miner, J. D'Andrilli, R. Mackelprang, et al., "Emergent Biogeochemical Risks From Arctic Permafrost Degradation," *Nature Climate Change* 11, no. 10 (2021): 809–819, https://doi.org/10.1038/s41558-021-01162-y.

80. K. Schaefer, Y. Elshorbany, E. Jafarov, et al., "Potential Impacts of Mercury Released From Thawing Permafrost," *Nature Communications* 11 (2020): 4650, https://doi.org/10.1038/s41467-020-18398-5.

81. R. M. Sebastian and J. Loui, "Waste Management in Northwest Territories, Canada: Current Practices, Opportunities, and Challenges," *Journal of Environmental Chemical Engineering* 10, no. 1 (2022): 106930, https://doi.org/10.1016/j.jece.2021.106930.

82. R. Landriau, C.R. Burn, T. Ensom, and C. Klengenberg, "Performance of Five Drilling Waste Sumps, Mackenzie Delta, Western Arctic Canada," in *Proceedings of the 12th International Conference on Permafrost*, eds R.A. Beddoe ansd K.C. Karunaratne (Ottawa, ON: International Permafrost Association, 2024); 200–208, https://doi.org/10.52381/ICOP2024.146.1.

83. M. Langer, T. S. von Deimling, S. Westermann, et al., "Thawing Permafrost Poses an Environmental Threat to Thousands of Sites With Legacy Industrial Contamination," *Nature Communications* 14 (2023): 1721, https://doi.org/10.1038/s41467-023-37276-4.

84. E. A. G. Schuur, A. D. McGuire, C. Schädel, et al., "Climate Change and the Permafrost Carbon Feedback," *Nature* 520, no. 7546 (2015): 171–179, https://doi.org/10.1038/nature14338.

85. K. S. Chin, J. Lento, J. M. Culp, D. Lacelle, and S. V. Kokelj, "Permafrost Thaw and Intense Thermokarst Activity Decreases Abundance of Stream Benthic Macroinvertebrates," *Global Change Biology* 22, no. 8 (2016): 2715–2728, https://doi.org/10.1111/gcb.13225.

86. J. A. O'Donnell, M. P. Carey, J. C. Koch, et al., "Metal Mobilization From Thawing Permafrost to Aquatic Ecosystems Is Driving Rusting of Arctic Streams," *Communications Earth & Environment* 5 (2024): 268, https://doi.org/10.1038/s43247-024-01446-z.

87. C. R. See, A.-M. Virkkala, S. M. Natali, et al., "Decadal Increases in Carbon Uptake Offset by Respiratory Losses Across Northern Permafrost Ecosystems," *Nature Climate Change* 14, no. 8 (2024): 853–862, https://doi.org/10.1038/s41558-024-02057-4.

88. S. M. Natali, J. D. Watts, B. M. Rodgers, et al., "Large Loss of CO_2 in Winter Observed Across the Northern Permafrost Region," *Nature Climate Change* 9, no. 11 (2019): 852–857, https://doi.org/10.1038/s41558-019-0592-8.

89. M. A. Kuhn, R. K. Varner, D. Bastviken, et al., "BAWLD-CH_4: A Comprehensive Dataset of Methane Fluxes From Boreal and Arctic Ecosystems," *Earth System Science Data* 13, no. 11 (2021): 5151–5189, https://doi.org/10.5194/essd-13-5151-2021.

90. M. R. Turetsky, B. W. Abbott, M. C. Jones, et al., "Carbon Release Through Abrupt Permafrost Thaw," *Nature Geoscience* 13, no. 2 (2020): 138–143, https://doi.org/10.1038/s41561-019-0526-0.

91. M. C. Mack, X. J. Walker, J. F. Johnstone, et al., "Carbon Loss From Boreal Forest Wildfires Offset by Increased Dominance of Deciduous Trees," *Science* 372, no. 6539 (2021): 280–283, https://doi.org/10.1126/science.abf3903.

92. S. E. Tank, J. W. McClelland, R. G. M. Spencer, et al., "Recent Trends in the Chemistry of Major Northern Rivers Signal Widespread Arctic Change," *Nature Geoscience* 16, no. 9 (2023): 789–796, https://doi.org/10.1038/s41561-023-01247-7.

93. P. C. Kemeny, G. K. Li, M. Douglas, et al., "Arctic Permafrost Thawing Enhances Sulfide Oxidation," *Global Biogeochemical Cycles* 37, no. 11 (2023): e2022GB007644, https://doi.org/10.1029/2022GB007644.

94. C. Hirst, A. Monhonval, E. Mauclet, et al., "Evidence for Late Winter Biogeochemical Connectivity in Permafrost Soils," *Communications Earth & Environment* 4 (2023): 85, https://doi.org/10.1038/s43247-023-00740-6.

95. A. Monhonval, J. Strauss, M. Thomas, et al., "Thermokarst Processes Increase the Supply of Stabilizing Surfaces and Elements (Fe, Mn, Al, and Ca) for Mineral-Organic Carbon Interactions," *Permafrost and Periglacial Processes* 33, no. 4 (2022): 452–469, https://doi.org/10.1002/ppp.2162.

96. M. Thomas, A. Monhonval, C. Hirst, et al., "Evidence for Preservation of Organic Carbon Interacting With Iron in Material Displaced From Retrogressive Thaw Slumps: Case Study in Peel Plateau, Western Canadian Arctic," *Geoderma* 433 (2023): 116443, https://doi.org/10.1016/j.geoderma.2023.116443.

97. A. G. Lim, M. Jiskra, J. E. Sonke, S. V. Loiko, N. Kosykh, and O. S. Pokrovsky, "A Revised Pan-Arctic Permafrost Soil Hg Pool Based on Western Siberian Peat Hg and Carbon Observations," *Biogeosciences* 17, no. 12 (2020): 3083–3097, https://doi.org/10.5194/bg-17-3083-2020.

98. S. Zolkos, D. P. Krabbenhoft, A. Suslova, et al., "Mercury Export From Arctic Great Rivers," *Environmental Science & Technology* 54, no. 7 (2020): 4140–4148, https://doi.org/10.1021/acs.est.9b07145.

99. A. J. Barker, T. D. Sullivan, W. B. Baxter, et al., "Iron Oxidation-Reduction Processes in Warming Permafrost Soils and Surface Waters Expose a Seasonally Rusting Arctic Watershed," *ACS Earth and Space Chemistry* 7, no. 8 (2023): 1479–1495, https://doi.org/10.1021/acsearthspacechem.2c00367.

100. E. K. Skierszkan, V. A. Schoepfer, M. D. Fellwock, et al., "Arsenic Mobilization Induced by Thawing Permafrost," *ACS Earth and Space Chemistry* 8, no. 4 (2024): 745–759, https://doi.org/10.1021/acsearthspacechem.3c00355.

101. E. K. Skierszkan, S. K. Carey, S. I. Jackson, M. Fellwock, C. Fraser, and M. B. J. Lindsay, "Seasonal Controls on Stream Metal(loid) Signatures in Mountainous Discontinuous Permafrost," *Science of the Total Environment* 908 (2024): 167999, https://doi.org/10.1016/j.scitotenv.2023.167999.

102. A. Runge, I. Nitze, and G. Grosse, "Remote Sensing Annual Dynamics of Rapid Permafrost Thaw Disturbances With LandTrendr," *Remote Sensing of Environment* 268, no. 1 (2022): 112752, https://doi.org/10.1016/j.rse.2021.112752.

103. F. M. Wagner, C. Mollaret, T. Günther, A. Kemna, and C. Hauck, "Quantitative Imaging of Water, Ice and Air in Permafrost Systems Through Petrophysical Joint Inversion of Seismic Refraction and Electrical Resistivity Data," *Geophysical Journal International* 219, no. 3 (2019): 1866–1875, https://doi.org/10.1093/gji/ggz402.

104. C. Mollaret, F. M. Wagner, C. Hilbich, C. Scapozza, and C. Hauck, "Petrophysical Joint Inversion Applied to Alpine Permafrost Field Sites to Image Subsurface Ice, Water, Air, and Rock Contents," *Frontiers in Earth Science* 8 (2020): 85, https://doi.org/10.3389/feart.2020.00085.

105. M. Farzamian, G. Blanchy, P. McLachlan, et al., "Advancing Permafrost Monitoring With Autonomous Electrical Resistivity Tomography (A-ERT): Low-Cost Instrumentation and Open-Source Data Processing Tool," *Geophysical Research Letters* 50, no. 6 (2023): e2023GL105770, https://doi.org/10.1029/2023GL105770.

106. T. Herring, A. Lewkowicz, C. Hauck, et al., "Best Practices for Using Electrical Resistivity Tomography to Investigate Permafrost," *Permafrost and Periglacial Processes* 34, no. 4 (2023): 494–512, https://doi.org/10.1002/ppp.2207.

107. J. Kunz, T. Ullman, C. Kneisel, and R. Baumhauer, "Three-Dimensional Subsurface Architecture and Its Influence on the Spatiotemporal Development of a Retrogressive Thaw Slump in the Richardson Mountains, Northwest Territories, Canada," *Arctic, Antarctic, and Alpine Research* 55, no. 1 (2023): 2167358, https://doi.org/10.1080/15230430.2023.2167358.

108. A. I. Kizyakov, S. Wetterich, F. Günther, et al., "Landforms and Degradation Pattern of the Batagay Thaw Slump, Northeastern Siberia," *Geomorphology* 420 (2023): 108501, https://doi.org/10.1016/j.geomorph.2022.108501.

109. R. H. Fraser, S. G. Leblanc, C. Prevost, and J. Van der Sluijs, "Towards Precise Drone-Based Measurement of Elevation Change in Permafrost Terrain Experiencing Thaw and Thermokarst," *Drone Systems and Applications* 10, no. 1 (2022): 406–426, https://doi.org/10.1139/dsa-2022-0036.

110. F. Bearzot, R. Garzonio, B. Di Mauro, et al., "Kinematics of an Alpine Rock Glacier From Multi-Temporal UAV Surveys and GNSS Data," *Geomorphology* 402 (2022): 108116, https://doi.org/10.1016/j.geomorph.2022.108116.

111. J. Van der Sluijs, E. Saiet, R. H. Fraser, S. V. Kokelj, and C. N. Bakelaar, "Validation of Beyond Visual-Line-Of-Sight Drone Photogrammetry for Terrain and Canopy Height Applications," *Remote Sensing Applications: Society and Environment* 35 (2024): 101266, https://doi.org/10.1016/j.rsase.2024.101266.

112. A. Bartsch, T. Strozzi, and I. Nitze, "Permafrost Monitoring From Space," *Surveys in Geophysics* 44 (2023): 1579–1613, https://doi.org/10.1007/s10712-023-09770-3.

113. E. E. Webb, A. K. Liljedahl, J. A. Cordeiro, M. M. Loranty, C. Witharana, and J. W. Lichstein, "Permafrost Thaw Drives Surface Water Decline Across Lake-Rich Regions of the Arctic," *Nature Climate Change* 12, no. 9 (2022): 841–846, https://doi.org/10.1038/s41558-022-01455-w.

114. I. Olthof, R. H. Fraser, J. van der Sluijs, and H. Travers-Smith, "Detecting Long-Term Arctic Surface Water Changes," *Nature Climate Change* 13, no. 11 (2023): 1191–1193, https://doi.org/10.1038/s41558-023-01836-9.

115. E. E. Webb, A. K. Liljedahl, M. M. Loranty, C. Witharana, and J. W. Lichstein, "Reply to Detecting Long-Term Arctic Surface Water Changes," *Nature Climate Change* 13, no. 11 (2023): 1194–1196, https://doi.org/10.1038/s41558-023-01837-8.

116. A. Bartsch, G. Pointner, I. Nitze, et al., "Expanding Infrastructure and Growing Anthropogenic Impacts Along Arctic Coasts," *Environmental Research Letters* 16, no. 11 (2021): 115013, https://doi.org/10.1088/1748-9326/ac3176.

117. C. Witharana, M. R. Udawalpola, A. S. Perera, et al., *Ice-Wedge Polygon Detection in Satellite Imagery From Pan-Arctic Regions, Permafrost Discovery Gateway, 2001–2021* (Santa Barbara, CA: Arctic Data Center, 2023), https://doi.org/10.18739/A2KW57K57.

118. C. Dai, I. M. Howat, J. van der Sluijs, et al., "Applications of ArcticDEM for Measuring Volcanic Dynamics, Landslides, Retrogressive Thaw Slumps, Snowdrifts, and Vegetation Heights," *Science of Remote Sensing* 9 (2024): 100130, https://doi.org/10.1016/j.srs.2024.100130.

119. A. Bertone, C. Barboux, X. Bodin, et al., "Incorporating InSAR Kinematics Into Rock Glacier Inventories: Insights From 11 Regions Worldwide," *Cryosphere* 16, no. 7 (2022): 2769–2792, https://doi.org/10.5194/tc-16-2769-2022.

120. P. Pandey, S. N. Ali, S. S. Das, and A. R. Khan, "Rock Glaciers of the Semi-Arid Northwestern Himalayas: Distribution, Characteristics, and Hydrological Significance," *Catena* 238 (2024): 107845, https://doi.org/10.1016/j.catena.2024.107845.

121. D. B. Jones, S. Harrison, K. Anderson, S. Shannon, and R. A. Betts, "Rock Glaciers Represent Hidden Water Stores in the Himalaya," *Science of the Total Environment* 793 (2021): 145368, https://doi.org/10.1016/j.scitotenv.2021.145368.

122. J. M. Wani, R. J. Thayyen, S. Gruber, C. S. P. Ojha, and D. Stumm, "Single-Year Thermal Regime and Inferred Permafrost Occurrence in the Upper Ganglass Catchment of the Cold-Arid Himalaya, Ladakh,

India," *Science of the Total Environment* 703 (2020): 134631, https://doi.org/10.1016/j.scitotenv.2019.134631.

123. A. R. Khan, S. Singh, P. Pandey, A. Bhardwaj, and S. N. Ali, "Modelling Permafrost Distribution in Western Himalaya Using Remote Sensing and Field Observations," *Remote Sensing* 13, no. 21 (2021): 4403, https://doi.org/10.3390/rs13214403.

124. I. P. Pradhan and D. P. Shukla, "Biennial Analysis of Probable Permafrost Distribution for Kullu District, North-West Himalaya Using Landsat 8 Satellite Data," *Land Degradation and Development* 35, no. 1 (2024): 360–377, https://doi.org/10.1002/ldr.4921.

125. C. R. Burn, M. Cooper, S. R. Morison, T. Pronk, and J. H. Calder, "The CFES Scientific Statement on Climate Change—Its Impacts in Canada, and the Critical Role of Earth Scientists in Mitigation and Adaptation," *Geoscience Canada* 48, no. 2 (2021): 59–72, https://doi.org/10.12789/geocanj.2021.48.173.

126. C. R. Burn, "The Response (1958 to 1997) of Permafrost and Near-Surface Ground Temperatures to Forest Fire, Takhini River Valley, Southern Yukon Territory," *Canadian Journal of Earth Sciences* 37, no. 6 (1998): 849–861, https://doi.org/10.1139/e97-105.

127. E. G. Devoie, J. R. Craig, R. F. Connon, and W. L. Quinton, "Taliks: A Tipping Point in Discontinuous Permafrost Degradation in Peatlands," *Water Resources Research* 55, no. 11 (2019): 9838–9857, https://doi.org/10.1029/2018WR024488.

128. D. Lacelle, D. A. Fisher, M. Verret, and W. Pollard, "Improved Prediction of Vertical Distribution of Ground Ice in Arctic-Antarctic Permafrost Sediments," *Communications Earth & Environment* 3 (2022): 31, https://doi.org/10.1038/s43247-022-00367-z.

129. A. Castagner, A. Brenning, S. Gruber, and S. V. Kokelj, "Vertical Distribution of Excess Ice in Icy Sediments and Its Statistical Estimation From Geotechnical Data (Tuktoyaktuk Coastlands and Anderson Plain, Northwest Territories)," *Arctic Science* 9, no. 2 (2023): 483–496, https://doi.org/10.1139/as-2021-004.

130. C. R. Burn, "Transactions of the International Permafrost Association: Number 1," *Permafrost and Periglacial Processes* 24, no. 2 (2013): 96–98, https://doi.org/10.1002/ppp.1781.

Supporting Information

Additional supporting information can be found online in the Supporting Information section.